

Phenomenology of semi-hard processes at the LHC

Francesco Giovanni Celiberto

francescogiovanni.celiberto@fis.unical.it



Università della Calabria & INFN-Cosenza
Italy



Instituto de Física Teórica UAM/CSIC
Spain



Wilhelm and Else Heraeus Physics School

QCD - Old Challenges and New Opportunities

Physikzentrum Bad Honnef (Deutschen Physikalischen Gesellschaft)

Bad Honnef (Köln, Deutschland)

September 24th - 30th, 2017



Outline

1 Introductory remarks

- QCD and semi-hard processes
- BFKL resummation
- Towards new analyses

2 Phenomenology

- Mueller–Navelet jet production
- Inclusive di-hadron production
- Multi-jet production
- Heavy-quark pair photoproduction

3 Conclusions & Outlook

Outline

1 Introductory remarks

- QCD and semi-hard processes
- BFKL resummation
- Towards new analyses

2 Phenomenology

- Mueller–Navelet jet production
- Inclusive di-hadron production
- Multi-jet production
- Heavy-quark pair photoproduction

3 Conclusions & Outlook

Motivation

High energies reachable at the LHC and at future colliders

- ◊ great opportunity in the search for long-waited signals of New Physics...
 - ◊ ...faultless chance to test Standard Model in unprecedented kinematic ranges
 - ◊ only 5% of Universe visible, but 99% of this visible matter described by **QCD**
 - ◊ duality between non-perturbative and perturbative aspects (**confinement** and **asymptotic freedom** concurrent properties) makes QCD a challenging sector surrounded by a broad and constant interest in its phenomenology

Motivation

High energies reachable at the LHC and at future colliders

- ◊ great opportunity in the search for long-waited signals of New Physics...
 - ◊ ...faultless chance to test Standard Model in unprecedented kinematic ranges
 - ◊ only 5% of Universe visible, but 99% of this visible matter described by **QCD**
 - ◊ duality between non-perturbative and perturbative aspects (**confinement** and **asymptotic freedom** concurrent properties) makes QCD a challenging sector surrounded by a broad and constant interest in its phenomenology

Semi-hard processes

Collision processes with the following **scale hierarchy**: $s \gg Q^2 \gg \Lambda_{\text{QCD}}^2$

- ◊ Q is the **hard scale** of the process (e.g. photon virtuality, heavy quark mass, jet/hadron transverse momentum, t , etc.)
 - ◊ large $Q \implies \alpha_s(Q) \ll 1 \implies$ perturbative QCD
 - ◊ large $s \implies$ large energy logs $\implies \alpha_s(Q) \log s \sim 1 \implies$ need to **resummation**

The BFKL resummation

pQCD, **semi-hard processes**: $s \gg Q^2 \gg \Lambda_{\text{QCD}}^2$

- ◊ Gluon quantum numbers in the t -channel: octet color representation, negative signature
 - ◊ Regge limit: $s \simeq -u \rightarrow \infty$, t not growing with s

- **BFKL resummation:** IV.S Fadin, EA Kuraev, L.N Lipatov (1975, 1976, 1977); I.Y Balitskii, L.N Lipatov (1978)

based on gluon Reggeization

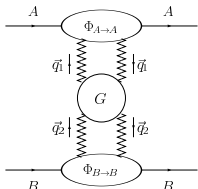
leading logarithmic approximation (LLA):

$$\alpha_c^n (\ln s)^n$$

next-to-leading logarithmic approximation (NLA)

$$\alpha_s^{n+1} (\ln s)^n$$

total cross section for $A + B \rightarrow X$: $\sigma_{AB}(s) = \frac{\Im m_s(\mathcal{A}_{AB}^{AB})}{s} \iff \text{optical theorem}$



► $\text{Im}_s(\mathcal{A}_{AB}^{AB})$ factorization

convolution of the **Green's function** of two interacting Reggeized gluons with the **impact factors** of the colliding particles.

$$\text{Im}_s(\mathcal{A}) = \frac{s}{(2\pi)^{D-2}} \int \frac{d^{D-2}q_1}{\vec{q}_1^2} \Phi_A(\vec{q}_1, \mathbf{s}_0) \int \frac{d^{D-2}q_2}{\vec{q}_2^2} \Phi_B(-\vec{q}_2, \mathbf{s}_0) \int_{\delta-i\infty}^{\delta+i\infty} \frac{d\omega}{2\pi i} \left(\frac{s}{\mathbf{s}_0}\right)^\omega G_\omega(\vec{q}_1, \vec{q}_2)$$

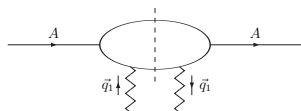
- **Green's function** is **process-independent** and takes care of the **energy dependence**

→ determined through the **BFKL equation**

[Ya.Ya. Balitskii, V.S. Fadin, E.A. Kuraev, L.N. Lipatov (1975)]

- **Impact factors** are **process-dependent** and depend on the hard scale, but not on the energy

→ known in the NLA just for few processes



- #### ◆ forward jet production

[J. Bartels, D. Colferai, G.P. Vacca (2003)]

(small-cone) IF. Caporale, D.Yu. Ivanov, B. Murdaca, A. Papa, A. Perri (2012))

(small-cone) [D.Yu. Ivanov, A. Papa (2012)]

(several jet algorithms discussed) [D. Colferai, A. Niccoli (2015)]

- ◆ forward identified hadron production

[D.Yu. Ivanov, A. Papa (2012)]

Towards new analyses

BFKL and Mueller–Navelet jets

So far, search for BFKL effects had these general drawbacks:

- ◊ too low \sqrt{s} or rapidity intervals among tagged particles in the final state
- ◊ too inclusive observables, other approaches can fit them

Advent of LHC:

- higher energies \leftrightarrow larger rapidity intervals
- unique opportunity to **test pQCD in the high-energy limit**
- disentangle applicability region of energy-log resummation (**BFKL approach**)

[V.S. Fadin, E.A. Kuraev, L.N. Lipatov (1975, 1976, 1977)]

[Y. Balitskii, L.N. Lipatov (1978)]

Last years:

Mueller–Navelet jets

- ◊ hadroproduction of two jets featuring high transverse momenta and well separated in rapidity
- ◊ possibility to define *infrared-safe* observables...
- ◊ ...and constrain the PDFs
- ◊ theory vs experiment

[B. Ducloué, L. Szymanowski, S. Wallon (2014)]
 [F. Caporale, D.Yu. Ivanov, B. Murdaca, A. Papa (2014)]

BFKL and Mueller–Navelet jets

So far, search for BFKL effects had these general drawbacks

- ◊ too low \sqrt{s} or rapidity intervals among tagged particles in the final state
 - ◊ too inclusive observables, other approaches can fit them

Advent of LHC:

- higher energies \leftrightarrow larger rapidity intervals
 - unique opportunity to **test pQCD in the high-energy limit**
 - disentangle applicability region of energy-log resummation (**BFKL approach**)

[V.S. Fadin, E.A. Kuraev, L.N. Lipatov (1975, 1976, 1977)]

[Y.Y. Balitskii, L.N. Lipatov (1978)]

Last years:

Mueller–Navelet jets

- ❖ hadroproduction of two jets featuring high transverse momenta and well separated in rapidity
 - ❖ possibility to define *infrared-safe* observables...
 - ❖ ...and constrain the PDFs
 - ❖ theory vs experiment

[B. Ducloué, L. Szymanowski, S. Wallon (2014)]
 [E. Caporale, D.Yu. Ivanov, B. Murdaca, A. Papa (2014)]

How could we further and deeply probe BFKL?

1. Study a less inclusive two-body final state...

Di-hadron production

[EG C., D.Yu. Ivanov, B. Murdaca, A. Papa (2016, 2017)]

- ◊ inclusive production of a pair of charged light hadrons well separated in rapidity
 - ◊ hadrons can be detected at the LHC at much smaller values of the transverse momentum than jets!
 - ◊ possibility to constrain not only the PDFs, but also the FFs!

2. Study three- and four-body final state processes...

Multi-jet production

[F. Caporale, F.G. C., G. Chachamis, A. Sabio Vera (2016)]; [F. Caporale, F.G. C., G. Chachamis, D. Gordo Gómez, A. Sabio Vera (2016, 2017)]

- ◊ demand the tagging of one or/and two further jets in more central regions of the detectors with a relative separation in rapidity from each other
 - ◊ definition of new, **suitable BFKL observables...**
 - ◊ ...in order to further investigate the azimuthal distribution of the final state

3. ...consider new opportunities!

Outline

1 Introductory remarks

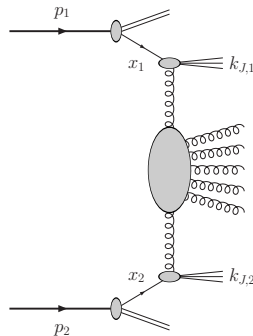
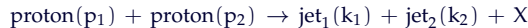
- QCD and semi-hard processes
- BFKL resummation
- Towards new analyses

2 Phenomenology

- Mueller–Navelet jet production
- Inclusive di-hadron production
- Multi-jet production
- Heavy-quark pair photoproduction

3 Conclusions & Outlook

Mueller-Navelet jets



- large jet transverse momenta (hard scales): $\vec{k}_1^2 \sim \vec{k}_2^2 \gg \Lambda_{\text{QCD}}^2$
- large rapidity gap between jets, $\Delta y \equiv Y = y_{J_1} - y_{J_2}$,
which requires large c.m. energy of the proton collisions, $s = 2p_1 \cdot p_2 \gg \vec{k}_{1,2}^2$

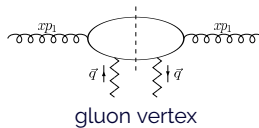
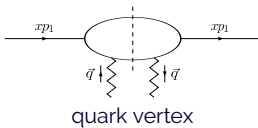
[A.H. Mueller, H. Navelet (1987)]

Forward jet impact factor

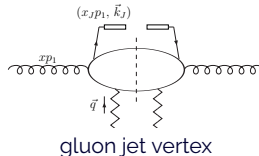
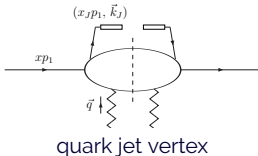
- take the impact factors for **colliding partons**

[V.S. Fadin, R. Fiore, M.I. Kotsky, A.P. (2000)]

[M. Ciafaloni and G. Rodrigo (2000)]



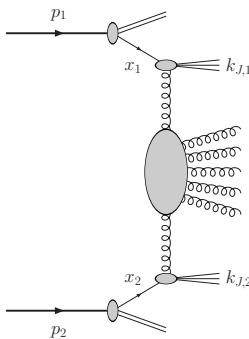
- "open" one of the integrations over the phase space of the intermediate state to allow one parton to generate the jet



- use QCD collinear factoriz.: $\sum_{s=q,\bar{q}} f_s \otimes [\text{quark vertex}] + f_g \otimes [\text{gluon vertex}]$

BFKL cross section (Mueller–Navelet jets)...

$$\frac{d\sigma}{dx_{J_1} dx_{J_2} d^2 k_{J_1} d^2 k_{J_2}} = \sum_{i,j=q,\bar{q},g} \int_0^1 dx_1 \int_0^1 dx_2 f_i(x_1, \mu) f_j(x_2, \mu) \frac{d\hat{\sigma}_{ij}(x_1 x_2 s, \mu)}{dx_{J_1} dx_{J_2} d^2 k_{J_1} d^2 k_{J_2}}$$



- ▶ slight change of variable in the final state
- ▶ project onto the eigenfunctions of the LO BFKL kernel, i.e. transfer from the reggeized gluon momenta to the (n, ν) -representation
- ▶ suitable definition of the **azimuthal coefficients**

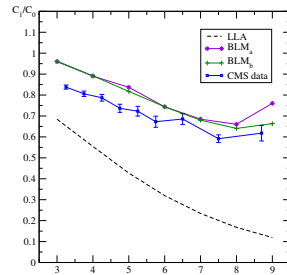
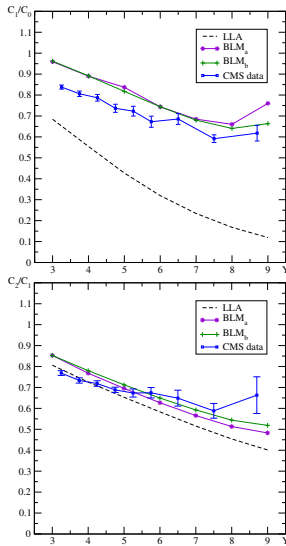
$$\frac{d\sigma}{dx_{J_1} dx_{J_2} d|\vec{k}_{J_1}| d|\vec{k}_{J_2}| d\phi_{J_1} d\phi_{J_2}} = \frac{1}{(2\pi)^2} \left[\mathcal{C}_0 + \sum_{n=1}^{\infty} 2 \cos(n\phi) \mathcal{C}_n \right]$$

with $\phi = \phi_{J_1} - \phi_{J_2} - \pi$

...useful definitions:

$$Y = \ln \frac{x_1 x_2 s}{|\vec{k}_{J_1}| |\vec{k}_{J_2}|}, \quad Y_0 = \ln \frac{s_0}{|\vec{k}_{J_1}| |\vec{k}_{J_2}|}$$

Theory versus experiment



$$R_{n0} \equiv C_n/C_0 = \langle \cos[n(\phi_{j_1} - \phi_{j_2} - \pi)] \rangle$$

$$R_{nm} \equiv C_n/C_m = R_{n0}/R_{m0}$$

vs $Y = y_{j_1} - y_{j_2}$

small-cone approximation

BLM scale setting

CMS (7 TeV; $|\vec{k}_1|, |\vec{k}_2| \geq 35 \text{ GeV}$)

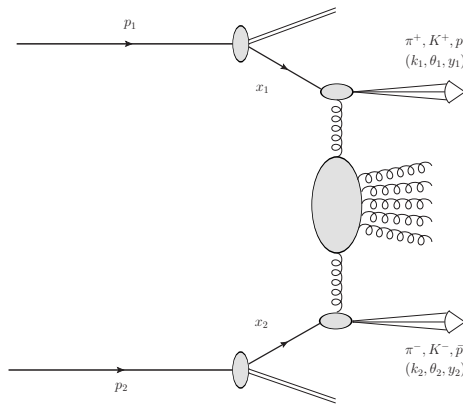
(7 TeV theory vs exp.) IF. Caporale, D.Yu. Ivanov, B. Murdaca, A. Papa (2014)

(7 TeV BFKL vs DGLAP + asym) IF.G. C., D.Yu. Ivanov, B. Murdaca, A. Papa (2015)

(13 TeV predictions + $C_0(Y)$) IF.G. C., D.Yu. Ivanov, B. Murdaca, A. Papa (2016)

Di-hadron production: theoretical setup

Process: $\text{proton}(p_1) + \text{proton}(p_2) \rightarrow h_1(k_1) + h_2(k_2) + X \quad \dots \text{LHC physics!}$



Di-hadron production

Process: proton(p_1) + proton(p_2) $\rightarrow h_1(k_1) + h_2(k_2) + X \dots LHC\ physics!$

$$\frac{d\sigma}{dy_1 dy_2 d^2 \vec{k}_1 d^2 \vec{k}_2} = \sum_{ij=qg} \int_0^1 \int dx_1 dx_2 f_i(x_1, \mu) f_j(x_2, \mu) \frac{d\hat{\sigma}(x_1 x_2 s, \mu)}{dy_1 dy_2 d^2 \vec{k}_1 d^2 \vec{k}_2}$$

- ◊ large hadron transverse momenta: $\vec{k}_1^2 \sim \vec{k}_2^2 \gg \Lambda_{QCD}^2 \Rightarrow pQCD\ allowed$
- ◊ QCD collinear factorization
- ◊ large rapidity intervals between hadrons (high energies) $\Rightarrow \Delta y = \ln \frac{x_1 x_2 s}{|\vec{k}_1||\vec{k}_2|}$
 \Rightarrow BFKL resummation: $\sum_n \left(a_n^{(0)} \alpha_s^n \ln^n s + a_n^{(1)} \alpha_s^n \ln^{n-1} s \right)$
- ◊ Collinear fragmentation of the parton i into a hadron h
 \Rightarrow convolution of D_i^h with a coefficient function C_i^h

$$d\sigma_i = C_i^h(z) dz \rightarrow d\sigma^h = d\alpha_h \int_{\alpha_h}^1 \frac{dz}{z} D_i^h \left(\frac{\alpha_h}{z}, \mu \right) C_i^h(z, \mu)$$

where α_h is the momentum fraction carried by the hadron

Di-hadron production: phenomenology

- Observables:

ϕ -averaged cross section \mathcal{C}_0 , $\langle \cos(n\phi) \rangle \equiv \frac{\mathcal{C}_n}{\mathcal{C}_0} \equiv R_{n0}$, with $n = 1, 2, 3$

$$\frac{\langle \cos(2\phi) \rangle}{\langle \cos(\phi) \rangle} \equiv \frac{\mathcal{C}_2}{\mathcal{C}_1} \equiv R_{21}, \quad \frac{\langle \cos(3\phi) \rangle}{\langle \cos(2\phi) \rangle} \equiv \frac{\mathcal{C}_3}{\mathcal{C}_2} \equiv R_{32}.$$

◆ *Integrated coefficients:*

$$C_n = \int_{y_{1,\min}}^{y_{1,\max}} dy_1 \int_{y_{2,\min}}^{y_{2,\max}} dy_2 \int_{k_{1,\min}}^{k_{1,\max}} dk_1 \int_{k_{2,\min}}^{k_{2,\max}} dk_2 \delta(y_1 - y_2 - Y) \mathcal{C}_n(y_1, y_2, k_1, k_2)$$

- Kinematic settings:

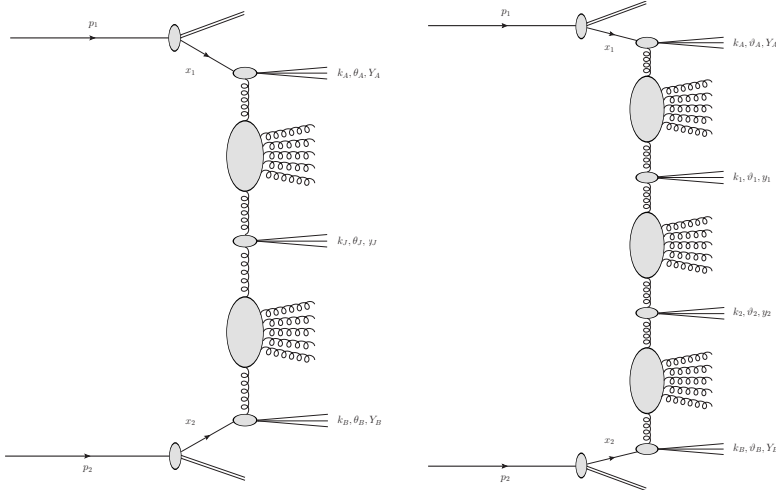
- ◊ $\sqrt{s} = 7, 13 \text{ TeV}$
 - ◊ $|y_i| \leq 2.4, 4.7$, with $i = 1, 2$
 - ◊ $k_{1,2} \geq 5 \text{ GeV}$...vs $k_{J_{1,2}}^{\text{MN-jets}} \geq 35 \text{ GeV!} \rightarrow$ more secondary gluon emissions!

● Phenomenological analysis:

- ◊ full **NLA** BFKL
 - ◊ (MSTW08, MMHT14, CT14) PDFs * (**AKK**, **DSS**, **HKNS**) FFs

[F.G. C., D.Yu Ivanov, B. Murdaca, A. Papa (2017)]

Three- and four-jet production



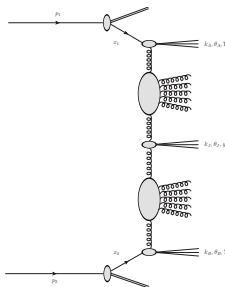
(Three-jets) [I.F. Caporale, G. Chachamis, B. Murdaca, A. Sabio Vera \(2015\)](#)
 (Three-jets) [I.F. Caporale, F.G. C., G. Chachamis, D. Gordo Gómez, A. Sabio Vera \(2016, 2017\)](#)
 (Four-jets) [I.F. Caporale, F.G. C., G. Chachamis, A. Sabio Vera \(2016\)](#)
 (Four-jets) [I.F. Caporale, F.G. C., G. Chachamis, D. Gordo Gómez, A. Sabio Vera \(2017\)](#)

Three-jet production...

The three-jet partonic cross section

Starting point: differential partonic cross-section (no PDFs)

$$\frac{d^3 \hat{\sigma}^{\text{3-jet}}}{dk_J d\theta_J dy_J} = \frac{\bar{\alpha}_s}{\pi k_J} \int d^2 \vec{p}_A \int d^2 \vec{p}_B \delta^{(2)}(\vec{p}_A + \vec{k}_J - \vec{p}_B) \\ \times \varphi(\vec{k}_A, \vec{p}_A, Y_A - y_J) \varphi(\vec{p}_B, \vec{k}_B, y_J - Y_B)$$



- Rapidity ordering: $Y_B < y_J < Y_A$
- k_J lie above the experimental resolution scale
- φ is the LO BFKL gluon Green function
- $\bar{\alpha}_s = \alpha_s N_c / \pi$

Three-jets: generalized azimuthal correlations

Prescription: integrate over all angles after using the projections on the two azimuthal angle differences indicated below...

→ ...to define:

$$\int_0^{2\pi} d\theta_A \int_0^{2\pi} d\theta_B \int_0^{2\pi} d\theta_J \cos(M(\theta_A - \theta_J - \pi)) \cos(N(\theta_J - \theta_B - \pi))$$

Main observables: **generalized azimuthal correlation momenta**

$$\mathcal{R}_{PQ}^{MN} = \frac{\mathcal{C}_{MN}}{\mathcal{C}_{PR}} = \frac{\langle \cos(M(\theta_A - \theta_J - \pi)) \cos(N(\theta_J - \theta_B - \pi)) \rangle}{\langle \cos(P(\theta_A - \theta_J - \pi)) \cos(Q(\theta_J - \theta_B - \pi)) \rangle}$$

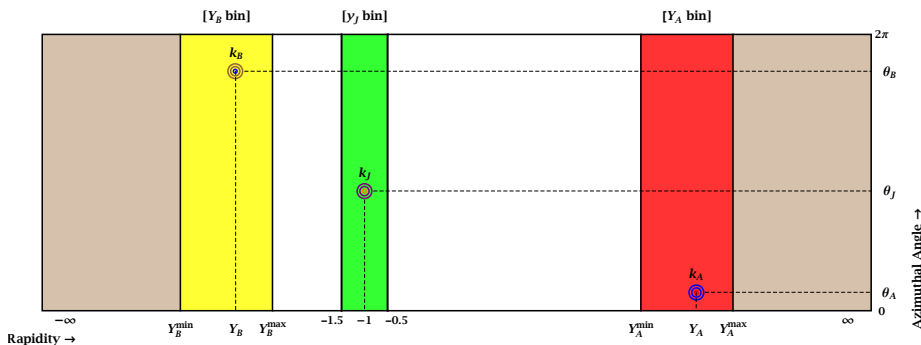
Remove the contribution from the zero conformal spin

to → drastically reduce the dependence on collinear configurations

study \mathcal{R}_{PQ}^{MN} with integer $M, N, P, Q > 0$

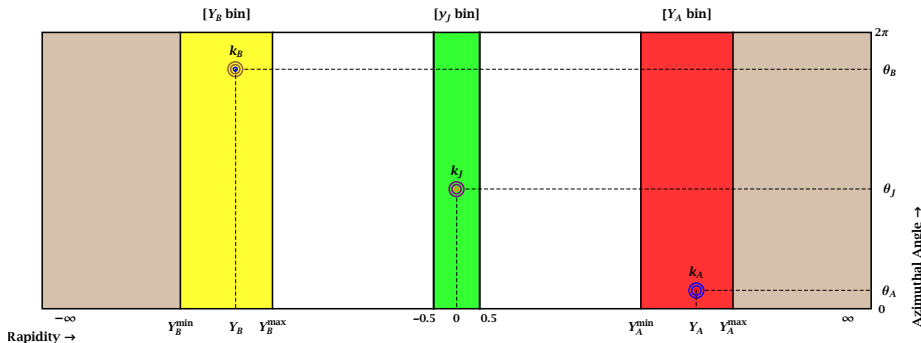
Next step: hadronic level predictions (PDFs + running α_s) to match LHC kinem. cuts

a) Integrate over a forward, backward and central rapidity bin



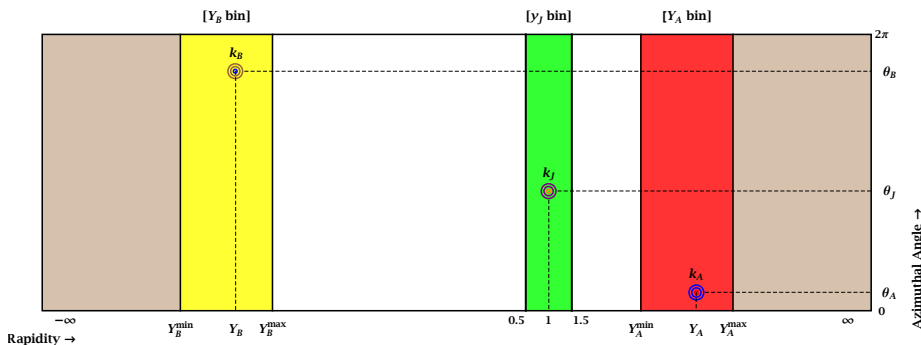
$$\begin{aligned} Y_A^{\max} &= -Y_B^{\min} = 4.7 \\ Y_A^{\min} &= -Y_B^{\max} = 3 \end{aligned}$$

a) Integrate over a forward, backward and central rapidity bin



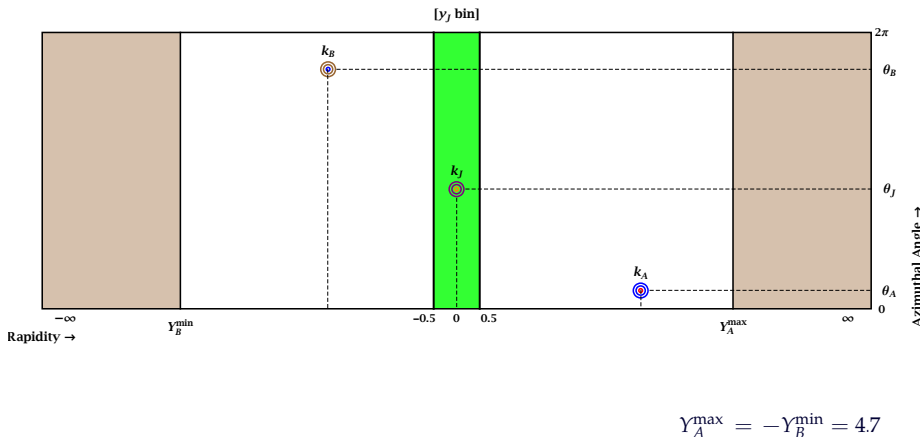
$$\begin{aligned} Y_A^{\max} &= -Y_B^{\min} = 4.7 \\ Y_A^{\min} &= -Y_B^{\max} = 3 \end{aligned}$$

a) Integrate over a forward, backward and central rapidity bin



$$\begin{aligned} Y_A^{\max} &= -Y_B^{\min} = 4.7 \\ Y_A^{\min} &= -Y_B^{\max} = 3 \end{aligned}$$

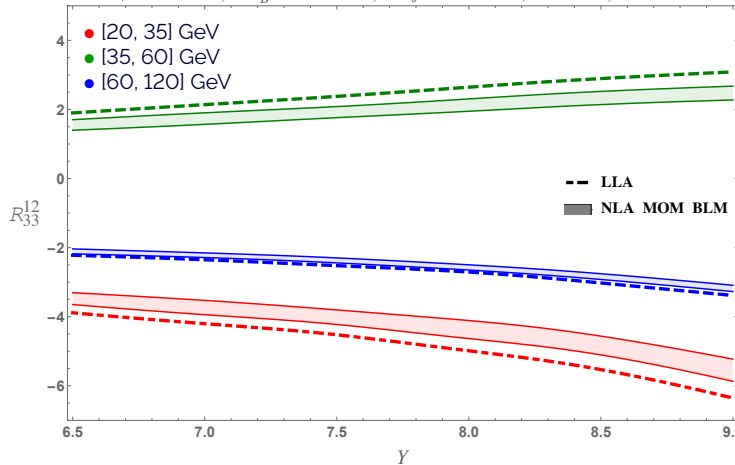
b) Integrate over a central rapidity bin



b) R_{33}^{12} vs γ at 7 TeV

$k_A^{\min} = 35 \text{ GeV}$, $k_B^{\min} = 50 \text{ GeV}$, $k_A^{\max} = k_B^{\max} = 60 \text{ GeV}$ (asymmetric)

$\sqrt{s} = 7 \text{ TeV}$; $k_B^{\min} = 50 \text{ GeV}$; $k_J \in$ ● bin-1, ● bin-2, ● bin-3

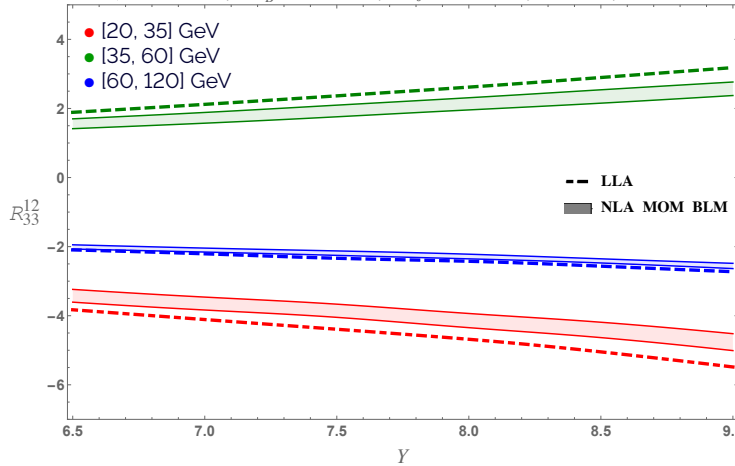


[F. Caporale, F.G. C., G. Chachamis, D. Gordo Gómez, A. Sabio Vera (2017)]

b) R_{33}^{12} vs γ at 13 TeV

$k_A^{\min} = 35 \text{ GeV}$, $k_B^{\min} = 50 \text{ GeV}$, $k_A^{\max} = k_B^{\max} = 60 \text{ GeV}$ (asymmetric)

$$\sqrt{s} = 13 \text{ TeV}; \quad k_B^{\min} = 50 \text{ GeV}; \quad k_J \in \bullet \text{ bin-1}, \bullet \text{ bin-2}, \bullet \text{ bin-3}$$



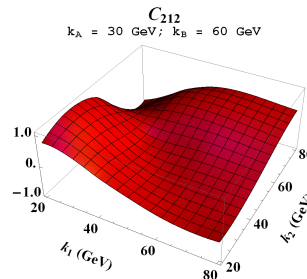
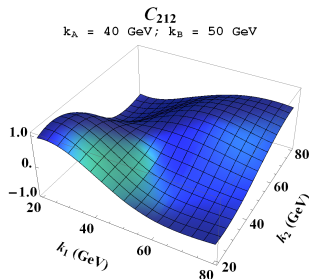
[F. Caporale, F.G. C., G. Chachamis, D. Gordo Gómez, A. Sabio Vera (2017)]

...four-jet production

Four-jets: generalized azimuthal correlations

As for the three-jet case...we define **generalized azimuthal correlation momenta**

$$\mathcal{R}_{PQR}^{MNL} = \frac{\mathcal{C}_{MNL}}{\mathcal{C}_{PRO}} = \frac{\langle \cos(M(\vartheta_A - \vartheta_1 - \pi)) \cos(N(\vartheta_1 - \vartheta_2 - \pi)) \cos(L(\vartheta_2 - \vartheta_B - \pi)) \rangle}{\langle \cos(P(\vartheta_A - \vartheta_1 - \pi)) \cos(Q(\vartheta_1 - \vartheta_2 - \pi)) \cos(R(\vartheta_2 - \vartheta_B - \pi)) \rangle}$$

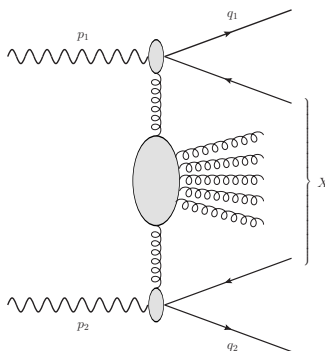


IF. Caporale, F.G. C., G. Chachamis, A. Sabio Vera (2016)
[F. Caporale, F.G. C., G. Chachamis, D. Gordo Gómez, A. Sabio Vera (2017)]

Heavy-quark pair photoproduction

Process: $\gamma(p_1) + \gamma(p_2) \rightarrow Q(q_1) + X + Q(q_2)$

... Q stands for a charm/bottom quark or antiquark



- photoproduction channel
- collision of (quasi-)real photons
- equivalent photon flux approximation
- quark masses play the role of hard scale
- first predictions within partial NLA BFKL
(NLA Green's function + LO impact factors)
 - ◊ LEP2 and future e^+e^- colliders
 - ◊ **ultra-peripheral (UPC)**
nucleus-nucleus (Pb-Pb) collisions at the LHC

[F.G. C., D.Yu. Ivanov, B. Murdaca, A. Papa (2017) [arXiv:1709.10032 \[hep-ph\]](https://arxiv.org/abs/1709.10032)]

Outline

1 Introductory remarks

- QCD and semi-hard processes
- BFKL resummation
- Towards new analyses

2 Phenomenology

- Mueller–Navelet jet production
- Inclusive di-hadron production
- Multi-jet production
- Heavy-quark pair photoproduction

3 Conclusions & Outlook

Conclusions...

- The **BFKL approach** offers a common basis for the description of *semi-hard processes*; it relies on a remarkable property of perturbative QCD, the **gluon Reggeization**
- Physical amplitudes in NLA are written in terms of a universal **Green's function** and of process-dependent **impact factors** of the colliding particles
- The number of reactions which can be investigated within NLA BFKL depends on the list of available NLO impact factors calculated so far
- Successful tests of NLA BFKL in the **Mueller–Navelet** channel with the advent of the LHC; nevertheless, *new BFKL-sensitive observables* as well as *more exclusive final-state reactions* are needed (**di-hadron**, **multi-jet**, **heavy-quark pair** production processes,...)

...Outlook

- ◊ Three- and four-jets in the full NLA BKFL
- ◊ Comparison with: fixed-order DGLAP predictions, Monte Carlo inspired calculations (all processes)
- ◊ Comparison higher-twist predictions: final-state objects stemming from (two) independent gluon ladders (MPI) (all processes)

(Mueller–Navelet jets) [R. Maciula, A. Szczurek (2014)]

(Mueller–Navelet jets) [B. Ducloué, L. Szymanowski, S. Wallon (2015)]

(Four-jets) [K. Kutak, R. Maciula, M. Serino, A. Szczurek, A. van Hameren (2016, 2016)]

- ◊ Inclusion of other resummation effects
- ◊ Probe the BFKL dynamics through other processes...
 - ▶ **hadron-jet** correlations:
FF dependence + asymmetric rapidity and transverse momenta ranges
 - ▶ **heavy-quark pair** production:
calculation of th NLO $q\bar{q}$ impact factor
photoproduction and heavy-ion UPC collisions
hadroproduction (process initiated by quarks and gluons)

[F.G. C., D.Yu. Ivanov, B. Murdaca, A. Papa (in progress)]

**Thanks for your
attention!!**

BACKUP slides

BACKUP slides

...and azimuthal coefficients (MN-jets)

$$\begin{aligned}\mathcal{C}_n = & \int_{-\infty}^{+\infty} d\nu e^{(Y-Y_0)[\bar{\alpha}_s(\mu_R)\chi(n,\nu)+\bar{\alpha}_s^2(\mu_R)K^{(1)}(n,\nu)]} \alpha_s^2(\mu_R) \\ & \times c_1(n,\nu) c_2(n,\nu) \left[1 + \alpha_s(\mu_R) \left(\frac{c_1^{(1)}(n,\nu)}{c_1(n,\nu)} + \frac{c_2^{(1)}(n,\nu)}{c_2(n,\nu)} \right) \right]\end{aligned}$$

where

$$\chi(n,\nu) = 2\Psi(1) - \Psi\left(\frac{n}{2} + \frac{1}{2} + i\nu\right) - \Psi\left(\frac{n}{2} + \frac{1}{2} - i\nu\right)$$

$$K^{(1)}(n,\nu) = \bar{\chi}(n,\nu) + \frac{\beta_0}{8N_c} \chi(n,\nu) \left(-\chi(n,\nu) + \frac{10}{3} + i \frac{d}{d\nu} \ln\left(\frac{c_1(n,\nu)}{c_2(n,\nu)}\right) + 2 \ln(\mu_R^2) \right)$$

$$c_1(n,\nu,|\vec{k}|,x) = 2\sqrt{\frac{C_F}{C_A}} (\vec{k}^2)^{i\nu-1/2} \left(\frac{C_A}{C_F} f_g(x, \mu_F) + \sum_{a=q,\bar{q}} f_a(x, \mu_F) \right)$$

...several NLA-equivalent expressions can be adopted for \mathcal{C}_n !

→ ...we use the *exponentiated* one

[F. Caporale, D.Yu Ivanov, B. Murdaca, A. Papa (2014)]

BACKUP slides

On the scale optimization: BLM method

NLA BFKL corrections to cross section with opposite sign with respect to the leading order (LO) result and large in absolute value...

- ◊ ...call for some optimization procedure...
- ◊ ...choose scales to mimic the most relevant subleading terms

- **BLM** [S.J. Brodsky, G.P. Lepage, P.B. Mackenzie (1983)]

- ✓ preserve the conformal invariance of an observable...
- ✓ ...by making vanish its β_0 -dependent part

* "Exact" BLM:

suppress NLO IFs + NLO Kernel β_0 -dependent factors

* Partial (approximated) BLM:

a) $(\mu_R^{BLM})^2 = k_1 k_2 \exp [2(1 + \frac{2}{3}I) - f(\nu) - \frac{5}{3}] \leftarrow \text{NLO IFs } \beta_0$

b) $(\mu_R^{BLM})^2 = k_1 k_2 \exp [2(1 + \frac{2}{3}I) - 2f(\nu) - \frac{5}{3} + \frac{1}{2}\chi(\nu, n)] \leftarrow \text{NLO Kernel } \beta_0$

$f(\nu)$ depends on the process

[F. Caporale, D.Yu. Ivanov, B. Murdaca, A. Papa (2015)]

BACKUP slides

MN-jets: the BFKL BLM cross section

a) $(\mu_R^{BLM})^2 = k_1 k_2 \exp [2(1 + \frac{2}{3}I) - f(\nu) - \frac{5}{3}] \sim 5^2 k_1 k_2$

b) $(\mu_R^{BLM})^2 = k_1 k_2 \exp [2(1 + \frac{2}{3}I) - 2f(\nu) - \frac{5}{3} + \frac{1}{2}\chi(\nu, n)] < (11.5)^2 k_1 k_2$

$$\mathcal{C}_n^{\text{BFKL(a)}} = \frac{x_{J_1} x_{J_2}}{|\vec{k}_{J_1}| |\vec{k}_{J_2}|} \int_{-\infty}^{+\infty} d\nu e^{(Y-Y_0)} \left[\bar{\alpha}_s(\mu_R) \chi(n, \nu) + \bar{\alpha}_s^2(\mu_R) \left(\bar{\chi}(n, \nu) - \frac{T^\beta}{C_A} \chi(n, \nu) - \frac{\beta_0}{8C_A} \chi^2(n, \nu) \right) \right]$$

$$\begin{aligned} & \times \alpha_s^2(\mu_R) c_1(n, \nu, |\vec{k}_{J_1}|, x_{J_1}) c_2(n, \nu, |\vec{k}_{J_2}|, x_{J_2}) \\ & \times \left[1 - \frac{2}{\pi} \alpha_s(\mu_R) T^\beta + \alpha_s(\mu_R) \left(\frac{\bar{c}_1^{(1)}(n, \nu, |\vec{k}_{J_1}|, x_{J_1})}{c_1(n, \nu, |\vec{k}_{J_1}|, x_{J_1})} + \frac{\bar{c}_2^{(1)}(n, \nu, |\vec{k}_{J_2}|, x_{J_2})}{c_2(n, \nu, |\vec{k}_{J_2}|, x_{J_2})} \right) \right] \end{aligned}$$

$$\begin{aligned} \mathcal{C}_n^{\text{BFKL(b)}} = & \frac{x_{J_1} x_{J_2}}{|\vec{k}_{J_1}| |\vec{k}_{J_2}|} \int_{-\infty}^{+\infty} d\nu e^{(Y-Y_0)} \left[\bar{\alpha}_s(\mu_R) \chi(n, \nu) + \bar{\alpha}_s^2(\mu_R) \left(\bar{\chi}(n, \nu) - \frac{T^\beta}{C_A} \chi(n, \nu) \right) \right] \\ & \times \alpha_s^2(\mu_R) c_1(n, \nu, |\vec{k}_{J_1}|, x_{J_1}) c_2(n, \nu, |\vec{k}_{J_2}|, x_{J_2}) \end{aligned}$$

$$\times \left[1 + \alpha_s(\mu_R) \left(\frac{\beta_0}{4\pi} \chi(n, \nu) - 2 \frac{T^\beta}{\pi} \right) + \alpha_s(\mu_R) \left(\frac{\bar{c}_1^{(1)}(n, \nu, |\vec{k}_{J_1}|, x_{J_1})}{c_1(n, \nu, |\vec{k}_{J_1}|, x_{J_1})} + \frac{\bar{c}_2^{(1)}(n, \nu, |\vec{k}_{J_2}|, x_{J_2})}{c_2(n, \nu, |\vec{k}_{J_2}|, x_{J_2})} \right) \right]$$

BACKUP slides

MN-jets: the DGLAP BLM cross section

$$a) \quad (\mu_R^{BLM})^2 = k_1 k_2 \exp [2(1 + \frac{2}{3}I) - f(\nu) - \frac{5}{3}] \sim 5^2 k_1 k_2$$

$$b) \quad (\mu_R^{BLM})^2 = k_1 k_2 \exp [2(1 + \frac{2}{3}I) - 2f(\nu) - \frac{5}{3} + \frac{1}{2}\chi(\nu, n)] < (11.5)^2 k_1 k_2$$

$$\mathcal{C}_n^{\text{DGLAP(a)}} = \frac{x_{J_1} x_{J_2}}{|\vec{k}_{J_1}| |\vec{k}_{J_2}|} \int_{-\infty}^{+\infty} d\nu \alpha_s^2(\mu_R) c_1(n, \nu, |\vec{k}_{J_1}|, x_{J_1}) c_2(n, \nu, |\vec{k}_{J_2}|, x_{J_2})$$

$$\times \left[1 - \frac{2}{\pi} \alpha_s(\mu_R) T^\beta + \bar{\alpha}_s(\mu_R) (Y - Y_0) \chi(n, \nu) \right. \\ \left. + \alpha_s(\mu_R) \left(\frac{\bar{c}_1^{(1)}(n, \nu, |\vec{k}_{J_1}|, x_{J_1})}{c_1(n, \nu, |\vec{k}_{J_1}|, x_{J_1})} + \frac{\bar{c}_2^{(1)}(n, \nu, |\vec{k}_{J_2}|, x_{J_2})}{c_2(n, \nu, |\vec{k}_{J_2}|, x_{J_2})} \right) \right]$$

$$\mathcal{C}_n^{\text{DGLAP(b)}} = \frac{x_{J_1} x_{J_2}}{|\vec{k}_{J_1}| |\vec{k}_{J_2}|} \int_{-\infty}^{+\infty} d\nu \alpha_s^2(\mu_R) c_1(n, \nu, |\vec{k}_{J_1}|, x_{J_1}) c_2(n, \nu, |\vec{k}_{J_2}|, x_{J_2})$$

$$\times \left[1 + \alpha_s(\mu_R) \left(\frac{\beta_0}{4\pi} \chi(n, \nu) - 2 \frac{T^\beta}{\pi} \right) + \bar{\alpha}_s(\mu_R) (Y - Y_0) \chi(n, \nu) \right. \\ \left. + \alpha_s(\mu_R) \left(\frac{\bar{c}_1^{(1)}(n, \nu, |\vec{k}_{J_1}|, x_{J_1})}{c_1(n, \nu, |\vec{k}_{J_1}|, x_{J_1})} + \frac{\bar{c}_2^{(1)}(n, \nu, |\vec{k}_{J_2}|, x_{J_2})}{c_2(n, \nu, |\vec{k}_{J_2}|, x_{J_2})} \right) \right]$$

BACKUP slides

MN-jets: the “exact” BLM cross section

$$\begin{aligned} \mathcal{C}_n^{\text{BLM}} = & \frac{x_{J_1} x_{J_2}}{|\vec{k}_{J_1}| |\vec{k}_{J_2}|} \int_{-\infty}^{+\infty} d\nu e^{(Y-Y_0)} \bar{\alpha}_s^{\text{MOM}}(\mu_R^{\text{BLM}}) \left[\chi(n, \nu) + \bar{\alpha}_s^{\text{MOM}}(\mu_R^{\text{BLM}}) \left(\bar{\chi}(n, \nu) + \frac{T^{\text{conf}}}{N_c} \chi(n, \nu) \right) \right] \\ & \times (\alpha_s^{\text{MOM}}(\mu_R^{\text{BLM}}))^2 c_1(n, \nu, |\vec{k}_{J_1}|, x_{J_1}) c_2(n, \nu, |\vec{k}_{J_2}|, x_{J_2}) \\ & \times \left[1 + \alpha_s^{\text{MOM}}(\mu_R^{\text{BLM}}) \left\{ \frac{\bar{c}_1^{(1)}(n, \nu, |\vec{k}_{J_1}|, x_{J_1})}{c_1(n, \nu, |\vec{k}_{J_1}|, x_{J_1})} + \frac{\bar{c}_2^{(1)}(n, \nu, |\vec{k}_{J_2}|, x_{J_2})}{c_2(n, \nu, |\vec{k}_{J_2}|, x_{J_2})} + \frac{2T^{\text{conf}}}{N_c} \right\} \right]. \end{aligned}$$

with the μ_R^{BLM} scale chosen as the solution of the following integral equation...

$$\begin{aligned} \mathcal{C}_n^\beta \equiv & \frac{x_{J_1} x_{J_2}}{|\vec{k}_{J_1}| |\vec{k}_{J_2}|} \int_{-\infty}^{\infty} d\nu \left(\frac{s}{s_0} \right)^{\bar{\alpha}_s^{\text{MOM}}(\mu_R^{\text{BLM}}) \chi(n, \nu)} \left(\alpha_s^{\text{MOM}}(\mu_R^{\text{BLM}}) \right)^3 \\ & \times c_1(n, \nu) c_2(n, \nu) \frac{\beta_0}{2N_c} \left[\frac{5}{3} + \ln \frac{(\mu_R^{\text{BLM}})^2}{Q_1 Q_2} - 2 \left(1 + \frac{2}{3} I \right) \right. \\ & \left. + \bar{\alpha}_s^{\text{MOM}}(\mu_R^{\text{BLM}}) \ln \frac{s}{s_0} \frac{\chi(n, \nu)}{2} \left(-\frac{\chi(n, \nu)}{2} + \frac{5}{3} + \ln \frac{(\mu_R^{\text{BLM}})^2}{Q_1 Q_2} - 2 \left(1 + \frac{2}{3} I \right) \right) \right] = 0 \end{aligned}$$

BACKUP slides

...choosing the μ_R^{BLM} scale (MN-jets)

...which represents the condition that terms proportional to β_0 in C_n disappear

$$\alpha^{\text{MOM}} = -\frac{\pi}{2T} \left[1 - \sqrt{1 + 4\alpha_s(\mu_R) \frac{T}{\pi}} \right],$$

with $T = T^\beta + T^{\text{conf}}$,

$$T^\beta = -\frac{\beta_0}{2} \left(1 + \frac{2}{3} I \right),$$

$$T^{\text{conf}} = \frac{C_A}{8} \left[\frac{17}{2} I + \frac{3}{2} (I-1) \xi + \left(1 - \frac{1}{3} I \right) \xi^2 - \frac{1}{6} \xi^3 \right].$$

where $I = -2 \int_0^1 dx \frac{\ln(x)}{x^2 - x + 1} \simeq 2.3439$ and ξ is a gauge parameter.

BACKUP slides

Observables and kinematics (MN-jets)

- **Observables:**

ϕ -averaged cross section \mathcal{C}_0 , $\langle \cos [n (\phi_{J_1} - \phi_{J_2} - \pi)] \rangle \equiv \frac{\mathcal{C}_n}{\mathcal{C}_0}$, with $n = 1, 2, 3$

$$\frac{\langle \cos [2 (\phi_1 - \phi_2 - \pi)] \rangle}{\langle \cos (\phi_1 - \phi_2 - \pi) \rangle} \equiv \frac{\mathcal{C}_2}{\mathcal{C}_1} \equiv R_{21}, \quad \frac{\langle \cos [3 (\phi_1 - \phi_2 - \pi)] \rangle}{\langle \cos [2 (\phi_1 - \phi_2 - \pi)] \rangle} \equiv \frac{\mathcal{C}_3}{\mathcal{C}_2} \equiv R_{32}.$$

- ◊ *Integrated coefficients:*

$$C_n = \int_{y_{1,\min}}^{y_{1,\max}} dy_1 \int_{y_{2,\min}}^{y_{2,\max}} dy_2 \int_{k_{J_1,\min}}^{\infty} dk_{J_1} \int_{k_{J_2,\min}}^{\infty} dk_{J_2} \delta (y_1 - y_2 - Y) \mathcal{C}_n (y_{J_1}, y_{J_2}, k_{J_1}, k_{J_2})$$

- **Kinematic settings:**

- ◊ $R = 0.5$ and $\sqrt{s} = 7, 13$ TeV
- ◊ $y_{\max}^C \leq |y_{J_{1,2}}| \leq 4.7$, with $y_{\max}^C = 0, 1.5 \simeq 4.7/3, 2.5$
- ◊ symmetric and **asymmetric** choices for k_{J_1} and k_{J_2} ranges

- **Numerical tools:** FORTRAN + NLO **MSTW08** PDFs + CERNLIB

[A.D. Martin, W.J. Stirling, R.S. Thorne, G. Watt (2009)]
<http://cernlib.web.cern.ch/cernlib>

BACKUP slides

High-energy DGLAP

- ◊ NLA BFKL expressions for the observables truncated to $\mathcal{O}(\alpha_s^3)$!

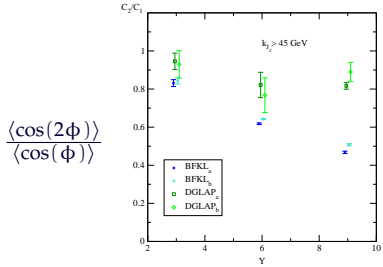
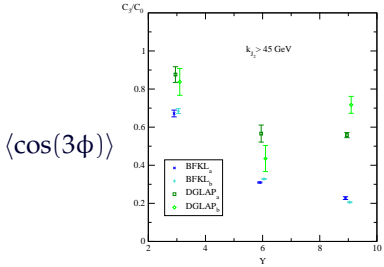
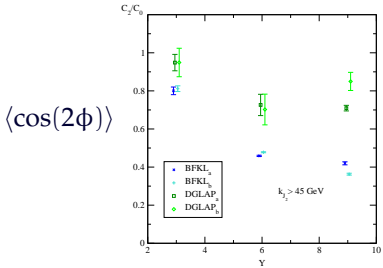
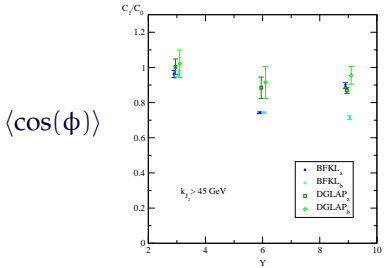
$$\begin{aligned} C_n^{DGLAP} = & \int_{-\infty}^{+\infty} d\nu \alpha_s^2(\mu_R) c_1(n, \nu) c_2(n, \nu) \\ & \times \left[1 + \bar{\alpha}_s(\mu_R) (Y - Y_0) \chi(n, \nu) + \alpha_s(\mu_R) \left(\frac{c_1^{(1)}(n, \nu)}{c_1(n, \nu)} + \frac{c_2^{(1)}(n, \nu)}{c_2(n, \nu)} \right) \right] \end{aligned}$$

Why asymmetric cuts?

- ▶ suppress Born contribution to ϕ -averaged cross section C_0 (back-to-back jets)
 - ◊ avoid instabilities observed in NLO fixed-order calculations
[J.R. Andersen, V. Del Duca, S. Frixione, C.R. Schmidt, W.J. Stirling (2001)]
[M. Fontannaz, J.P. Guillet, G. Heinrich (2001)]
 - ◊ **enhance effects of additional hard gluons** $\xrightarrow{\text{emphasize}}$ **BFKL effects**
- ▶ violation of energy-momentum in NLA strongly suppressed respect to LLA
[B. Ducloué, L. Szymanowski, S. Wallon (2014)]

BACKUP slides

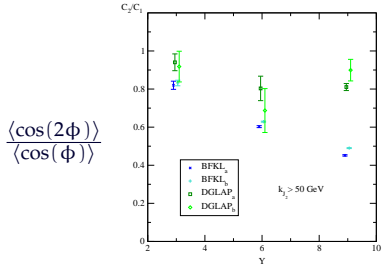
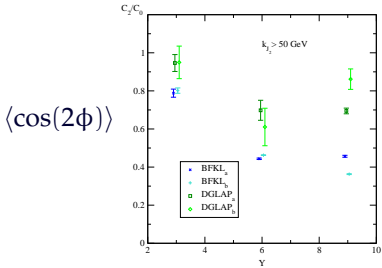
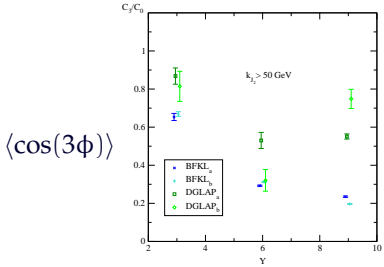
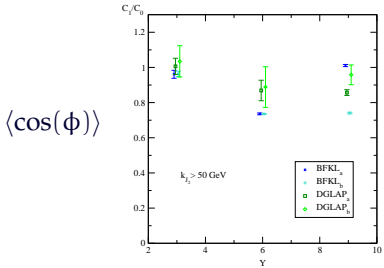
R_{nm} for $k_{J_1} > 35 \text{ GeV}, k_{J_2} > 45 \text{ GeV}$ at $\sqrt{s} = 7 \text{ TeV}$



[F.G. C., D.Yu. Ivanov, B. Murdaca, A. Papa (2015)]

BACKUP slides

R_{nm} for $k_{J_1} > 35 \text{ GeV}, k_{J_2} > 50 \text{ GeV}$ at $\sqrt{s} = 7 \text{ TeV}$



[F.G. C., D.Yu. Ivanov, B. Murdaca, A. Papa (2015)]

BACKUP slides

Exclusion of central jet rapidities (MN-jets)

Motivation...

- ◊ At given $Y = y_{J_1} - y_{J_2} \dots$
- $|y_{J_i}|$ could be so small ($\lesssim 2$), that the jet i is actually produced in the central region, rather than in one of the two forward regions
- longitudinal momentum fractions of the parent partons $x \sim 10^{-3}$
- for $|y_{J_i}|$ and $|k_{T,i}| < 100$ GeV \Rightarrow increase of C_0 by 25% due to NNLO PDF effects
[J. Currie, A. Gehrmann-De Ridder, E. W. N. Glover, J. Pires (2014)]
- ! Our BFKL description of the process could be not so accurate...

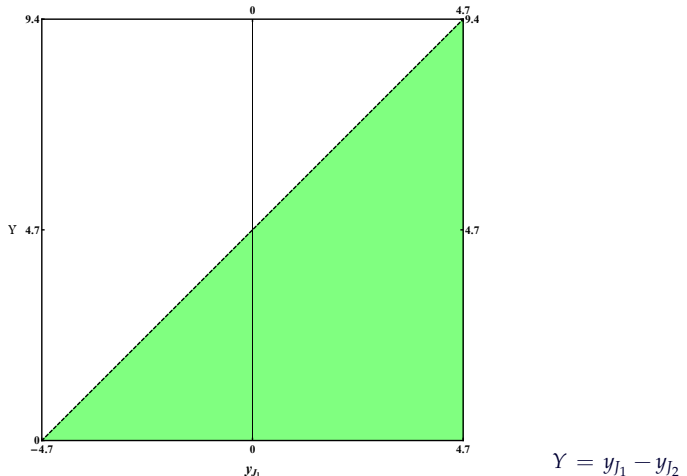
...let's return to the original Mueller–Navelet idea!

- ◊ remove regions where jets are produced at central rapidities...
- ...in order to reduce as much as possible theoretical uncertainties

BACKUP slides

Rapidity range (MN-jets)

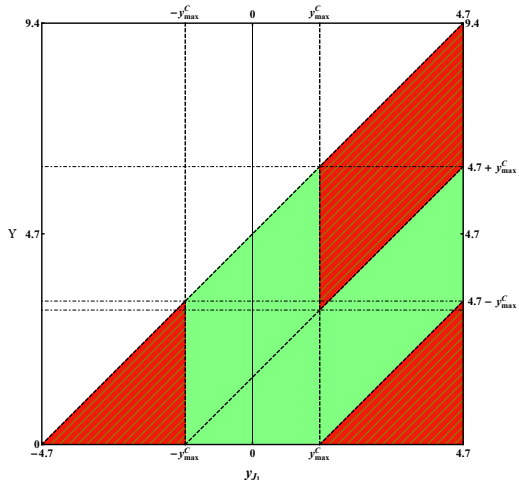
$$\int_{-4.7}^{4.7} dy_1 \int_{-4.7}^{4.7} dy_2 \delta(\mathbf{y}_1 - \mathbf{y}_2 - \mathbf{Y}) \theta(|y_1| - y_{\max}^C) \theta(|y_2| - y_{\max}^C) C_n(y_{J_1}, y_{J_2}, \mathbf{k}_{J_1}, \mathbf{k}_{J_2})$$



BACKUP slides

Rapidity range (MN-jets)

$$\int_{-4.7}^{4.7} dy_1 \int_{-4.7}^{4.7} dy_2 \delta(y_1 - y_2 - Y) \theta(|y_1| - y_{\max}^C) \theta(|y_2| - y_{\max}^C) C_n(y_{J_1}, y_{J_2}, k_{J_1}, k_{J_2})$$

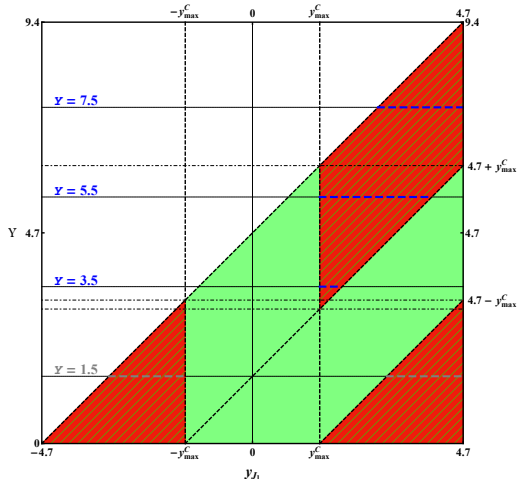


$$Y = y_{J_1} - y_{J_2}$$

BACKUP slides

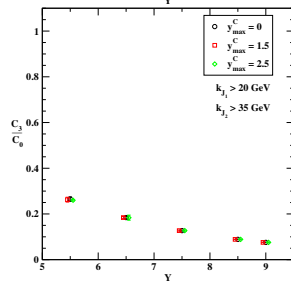
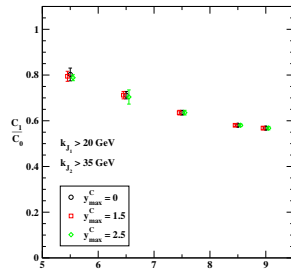
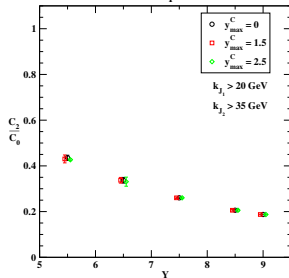
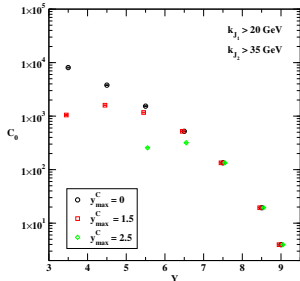
Rapidity range (MN-jets)

$$\int_{-4.7}^{4.7} dy_1 \int_{-4.7}^{4.7} dy_2 \delta(y_1 - y_2 - Y) \theta(|y_1| - y_{\max}^C) \theta(|y_2| - y_{\max}^C) C_n(y_{J_1}, y_{J_2}, k_{J_1}, k_{J_2})$$



BACKUP slides

R_{nm} for $k_{J_1} > 20$ GeV, $k_{J_2} > 35$ GeV at $\sqrt{s} = 13$ TeV



[F.G. C., D.Yu. Ivanov, B. Murdaca, A. Papa (2016)]

BACKUP slides

C_0 vs $Y = y_{J_1} - y_{J_2}$ - "exact" MOM BLM method

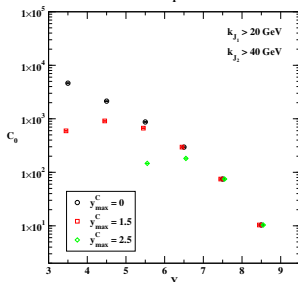
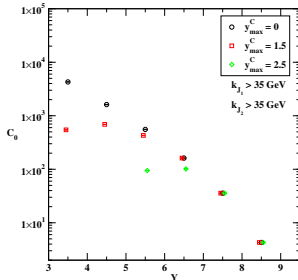
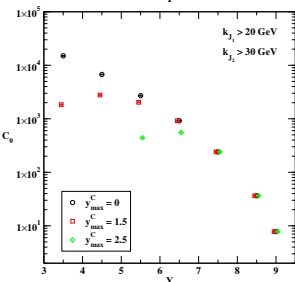
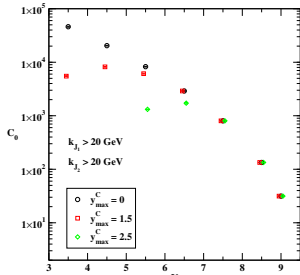


[FIG. C, DYU, Ivanov, B. Murdaca, A. Papa (2016)]

BACKUP slides

C_1/C_0 vs Y - "exact" BLM method

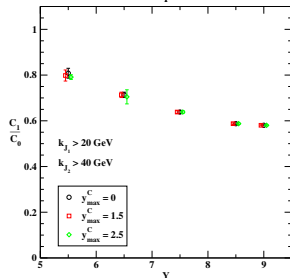
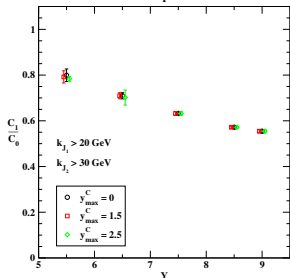
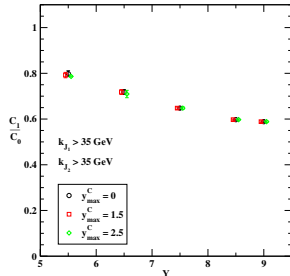
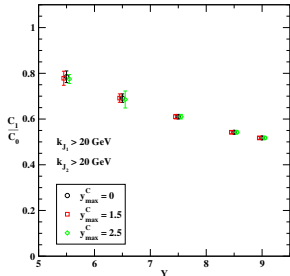


[FIG. C, D.Yu. Ivanov, B. Murdaca, A. Papa (2016)]

BACKUP slides

C_2/C_0 vs Y - "exact" BLM method

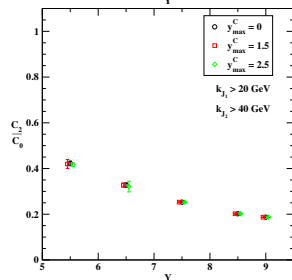
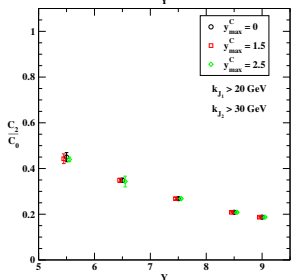
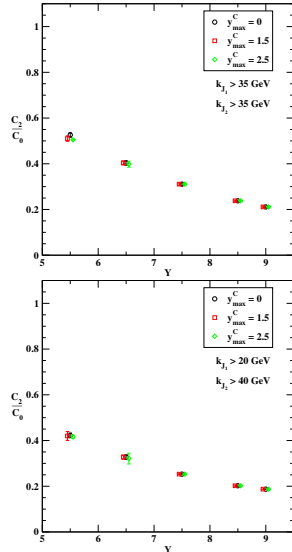
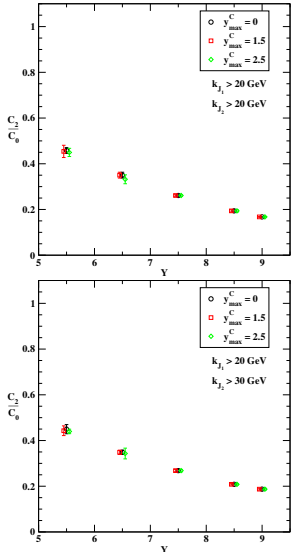


[FIG. C, D.Yu. Ivanov, B. Murdaca, A. Papa (2016)]

BACKUP slides

C_3/C_0 vs Y - "exact" BLM method

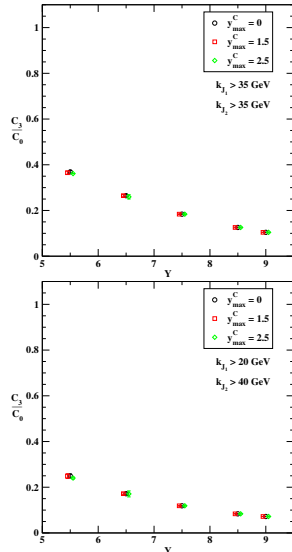
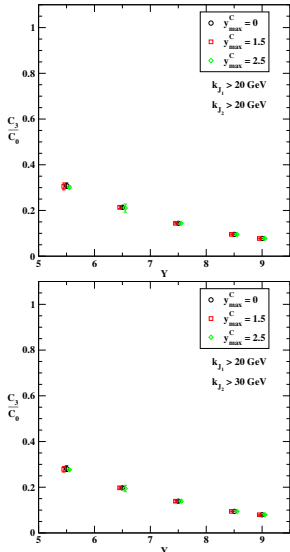


[FIG. C, D.Yu. Ivanov, B. Murdaca, A. Papa (2016)]

BACKUP slides

C_2/C_1 vs Y - "exact" BLM method

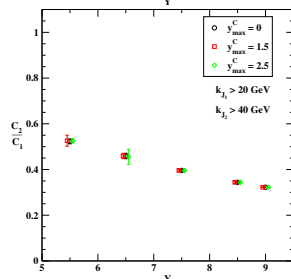
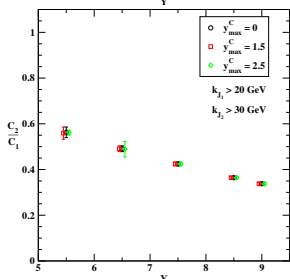
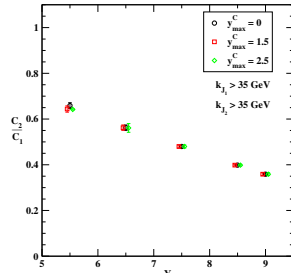
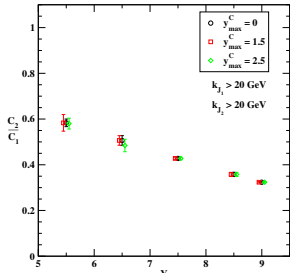


[FIG. C, D.Yu. Ivanov, B. Murdaca, A. Papa (2016)]

BACKUP slides

C_3/C_2 vs Y - "exact" BLM method

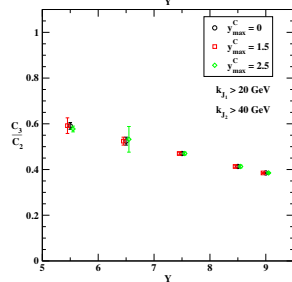
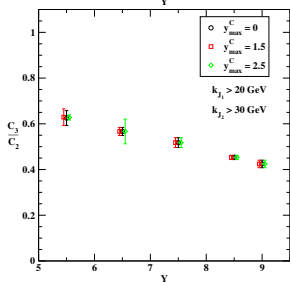
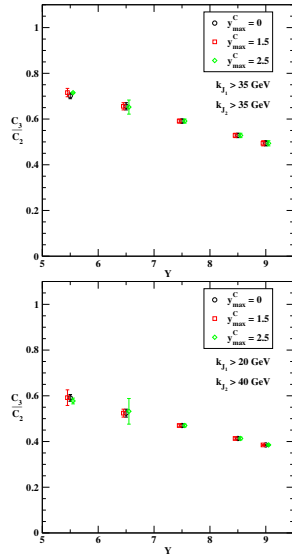
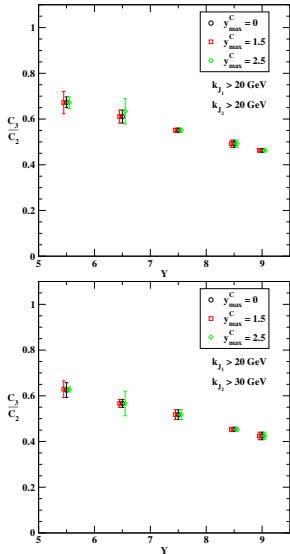
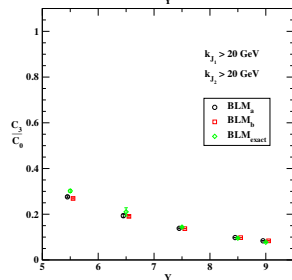
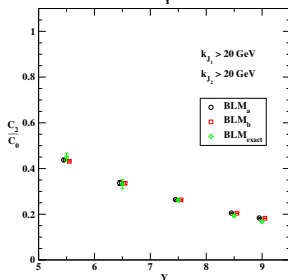
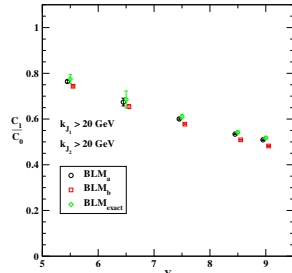
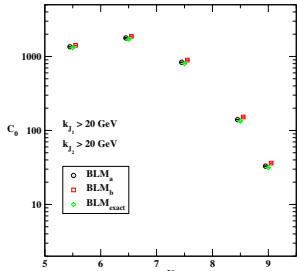


[FIG. C, D.Yu. Ivanov, B. Murdaca, A. Papa (2016)]

BACKUP slides

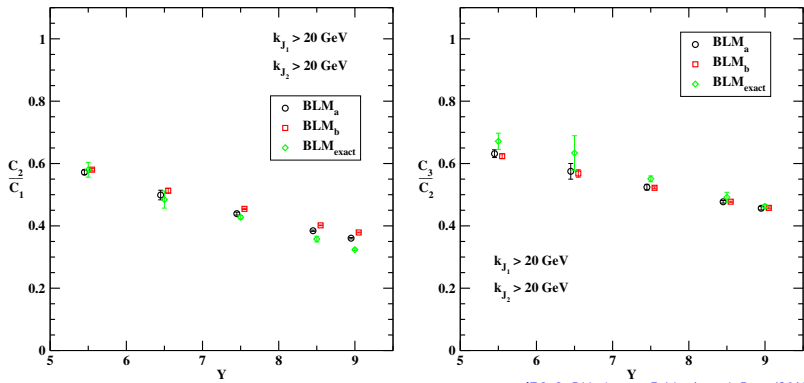
BLM comparisons of C_0 and R_{n0} vs γ - $y_{\max}^C = 2.5$



[F.G. C., D.Yu. Ivanov, B. Murdaca, A. Papa (2016)]

BACKUP slides

BLM comparisons of C_2/C_1 and C_3/C_2 vs γ - $y_{\max}^C = 2.5$



[F.G. C., D.Yu. Ivanov, B. Murdaca, A. Papa (2016)]

BACKUP slides

The BFKL BLM cross section (di-hadrons)

$$\begin{aligned} C_n^{\text{BLM}} = & \frac{e^Y}{s} \int_{y_{\min}}^{y_{\max}} dy_1 \int_{k_{1,\min}}^{\infty} dk_1 \int_{k_{2,\min}}^{\infty} dk_2 \int_{-\infty}^{+\infty} d\nu \exp \left[(Y - Y_0) \bar{\alpha}_s^{\text{MOM}}(\mu_R^*) \left\{ \chi(n, \nu) \right. \right. \\ & + \left. \left. \bar{\alpha}_s^{\text{MOM}}(\mu_R^*) \left(\bar{\chi}(n, \nu) + \frac{T^{\text{conf}}}{C_A} \chi(n, \nu) \right) \right\} \right] 4 (\alpha_s^{\text{MOM}}(\mu_R^*))^2 \frac{C_F}{C_A} \frac{1}{|\vec{k}_1| |\vec{k}_2|} \left(\frac{\vec{k}_1^2}{\vec{k}_2^2} \right)^{i\nu} \\ & \times \int_{\alpha_1}^1 \frac{dx}{x} \left(\frac{x}{\alpha_1} \right)^{2i\nu-1} \left[\frac{C_A}{C_F} f_g(x) D_g^h \left(\frac{\alpha_1}{x} \right) + \sum_{a=q,\bar{q}} f_a(x) D_a^h \left(\frac{\alpha_1}{x} \right) \right] \\ & \times \int_{\alpha_2}^1 \frac{dz}{z} \left(\frac{z}{\alpha_2} \right)^{-2i\nu-1} \left[\frac{C_A}{C_F} f_g(z) D_g^h \left(\frac{\alpha_2}{z} \right) + \sum_{a=q,\bar{q}} f_a(z) D_a^h \left(\frac{\alpha_2}{z} \right) \right] \\ & \times \left[1 + \bar{\alpha}_s^{\text{MOM}}(\mu_R^*) \left(\frac{\bar{c}_1^{(1)}(n, \nu)}{c_1(n, \nu)} + \frac{\bar{c}_2^{(1)}(n, \nu)}{c_2(n, \nu)} + 2 \frac{T^{\text{conf}}}{C_A} \right) \right], \end{aligned}$$

with the μ_R^* scale chosen as the solution of the following integral equation...

BACKUP slides

Numerical specifics (di-hadrons)

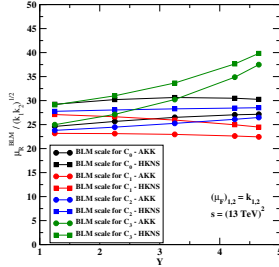
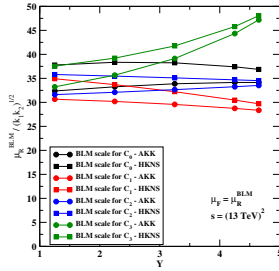
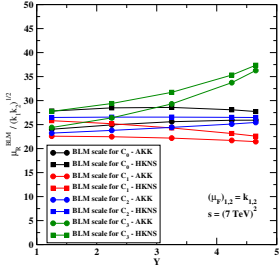
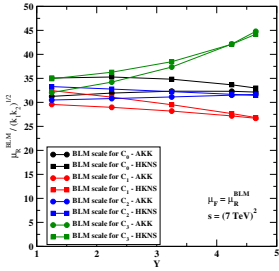
- Numerical tools:

FORTRAN → weak time dependence on multidim. integration ranges

- + NLO **MSTW08** PDFs (comparison with **MMHT14** and **CTEQ14**)
[A.D. Martin, W.J. Stirling, R.S. Thorne, G. Watt, (2009)]
- + three different FF parameterizations!
 - ▶ **AKK**
[S. Albino, B.A. Kniehl, G. Kramer, (2008)]
 - ▶ **DSS**
[D. de Florian, R. Sassot, M. Stratmann, (2007)]
 - ▶ **HKNS**
[M. Hirai, S. Kumano, T.-H. Nagai, K. Sudoh, (2007)]
- + **CERNLIB**
<http://cernlib.web.cern.ch/cernlib>

BACKUP slides

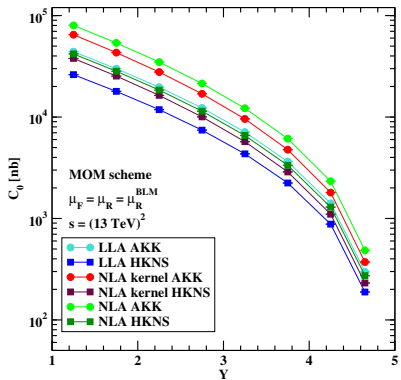
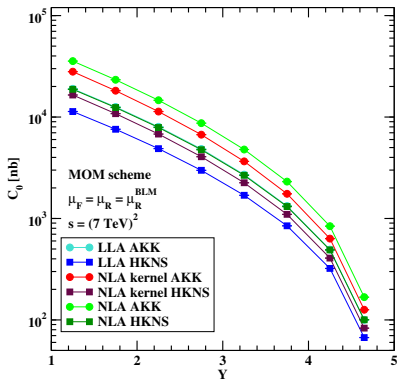
BLM values for μ_R (di-hadrons)



[F.G. C., D.Yu. Ivanov, B. Murdaca, A. Papa (2017)]

BACKUP slides

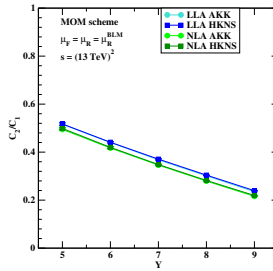
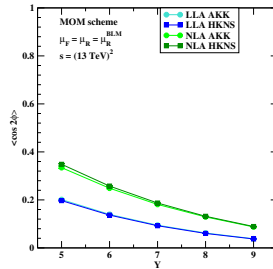
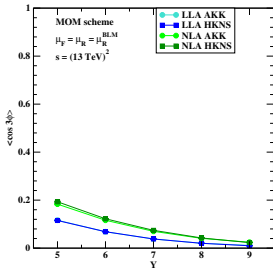
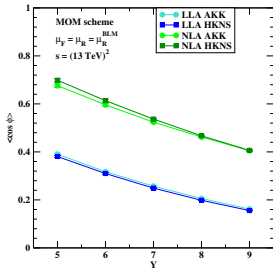
C_0 at $\sqrt{s} = 7, 13 \text{ TeV}$, $Y \leq 4.8$, $\mu_F = \mu_R^{\text{BLM}}$



I.F.G. C., D.Yu. Ivanov, B. Murdaca, A. Papa (2017)

BACKUP slides

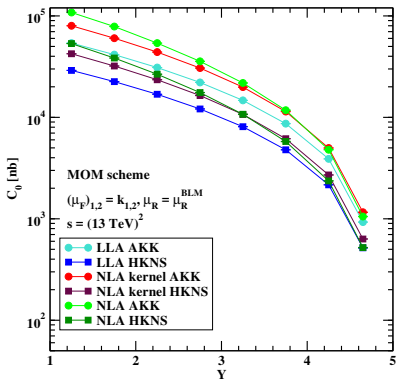
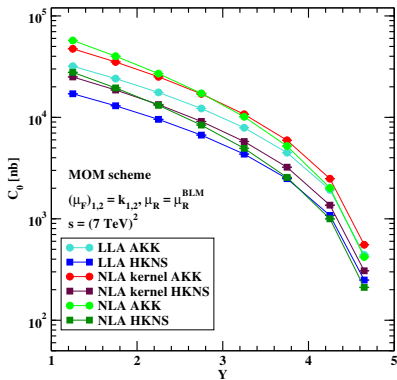
R_{nm} at $\sqrt{s} = 13 \text{ TeV}$, $Y \leq 9.4$, $\mu_F = \mu_R^{\text{BLM}}$



[F.G. C., D.Yu. Ivanov, B. Murdaca, A. Papa (2017)]

BACKUP slides

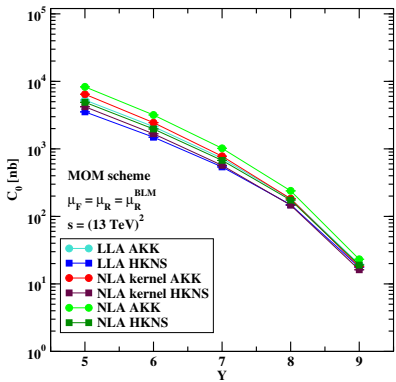
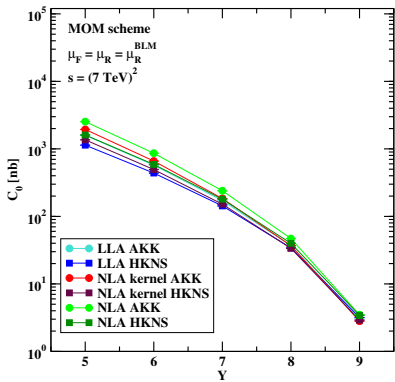
C_0 at $\sqrt{s} = 7, 13 \text{ TeV}$, $Y \leqslant 4.8$, $(\mu_F)_{1,2} = |\vec{k}_{1,2}|$



I.F.G. C., D.Yu. Ivanov, B. Murdaca, A. Papa (2017)

BACKUP slides

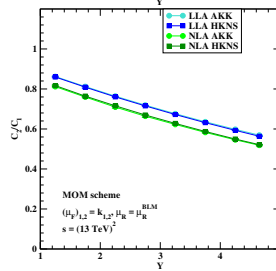
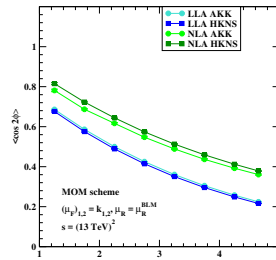
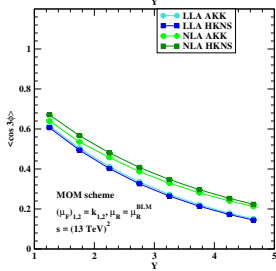
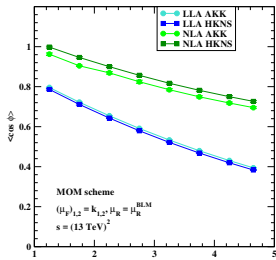
C_0 at $\sqrt{s} = 7, 13 \text{ TeV}$, $Y \leq 9.4$, $\mu_F = \mu_R^{\text{BLM}}$



I.F.G. C., D.Yu. Ivanov, B. Murdaca, A. Papa (2017)

BACKUP slides

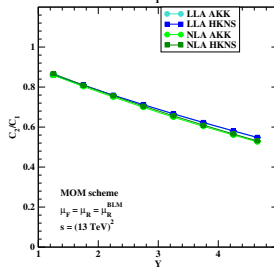
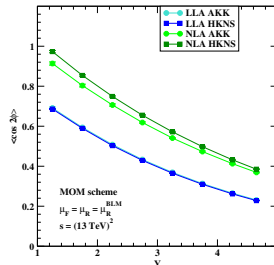
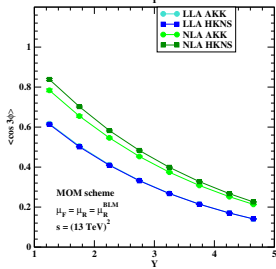
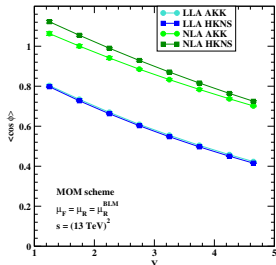
R_{nm} at $\sqrt{s} = 13 \text{ TeV}$, $Y \leq 4.8$, $(\mu_F)_{1,2} = |\vec{k}_{1,2}|$



[F.G. C., D.Yu. Ivanov, B. Murdaca, A. Papa (2017)]

BACKUP slides

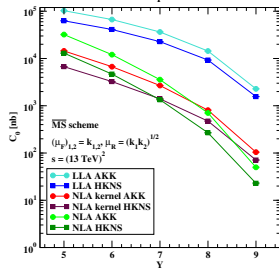
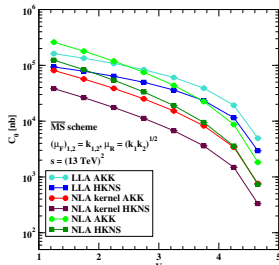
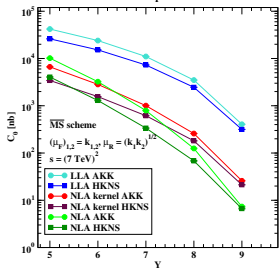
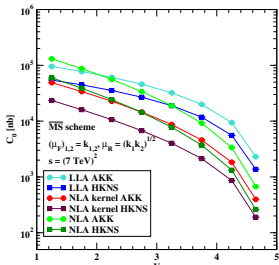
R_{nm} at $\sqrt{s} = 13 \text{ TeV}$, $Y \leq 4.8$, $\mu_F = \mu_R^{\text{BLM}}$



[F.G. C., D.Yu. Ivanov, B. Murdaca, A. Papa (2017)]

BACKUP slides

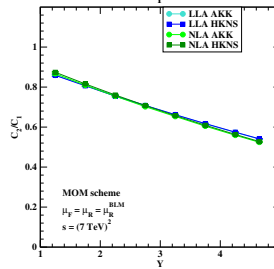
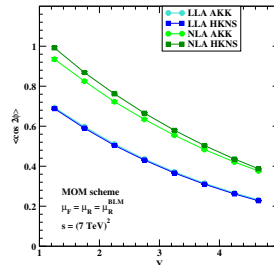
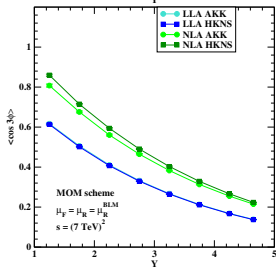
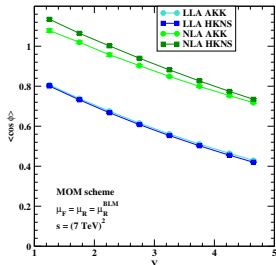
$$C_0 \text{ at } \sqrt{s} = 7, 13 \text{ TeV}, \mu_R = \sqrt{|\vec{k}_1||\vec{k}_2|}, (\mu_F)_{1,2} = |\vec{k}_{1,2}|$$



[F.G. C., D.Yu. Ivanov, B. Murdaca, A. Papa (2017)]

BACKUP slides

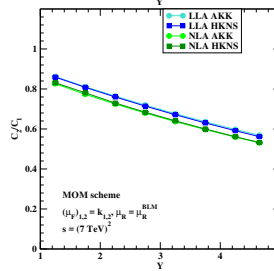
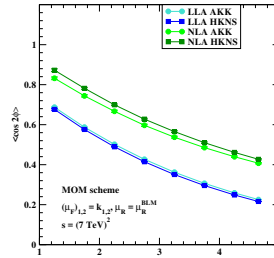
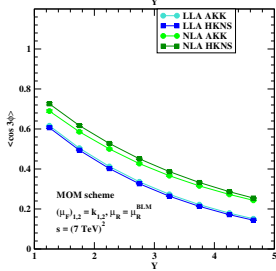
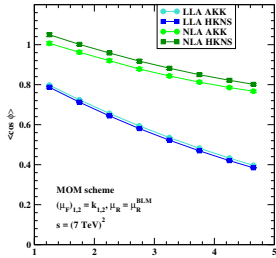
R_{nm} at $\sqrt{s} = 7 \text{ TeV}$, $Y \leq 4.8$, $\mu_F = \mu_R^{\text{BLM}}$



[F.G. C., D.Yu. Ivanov, B. Murdaca, A. Papa (2017)]

BACKUP slides

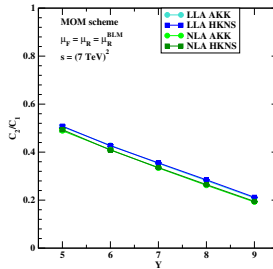
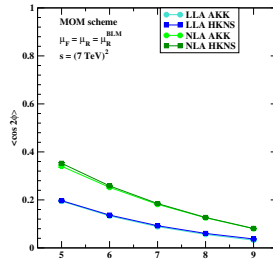
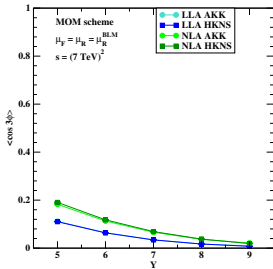
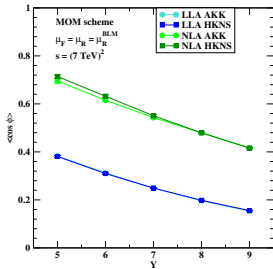
R_{nm} at $\sqrt{s} = 7 \text{ TeV}$, $Y \leq 4.8$, $(\mu_F)_{1,2} = |\vec{k}_{1,2}|$



[F.G.C., D.Yu. Ivanov, B. Murdaca, A. Papa (2017)]

BACKUP slides

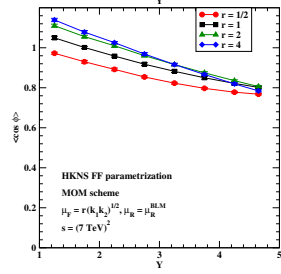
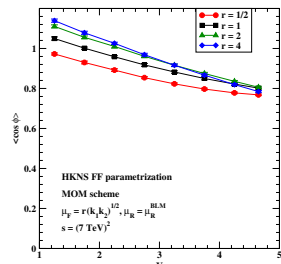
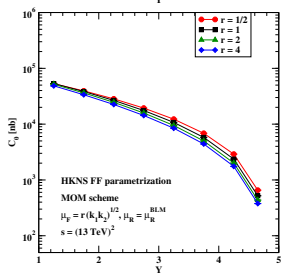
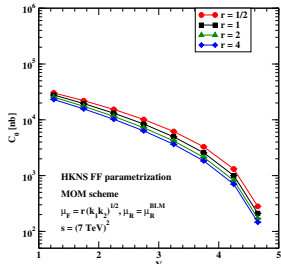
R_{nm} at $\sqrt{s} = 7 \text{ TeV}$, $Y \leq 9.4$, $\mu_F = \mu_R^{\text{BLM}}$



[F.G. C., D.Yu. Ivanov, B. Murdaca, A. Papa (2017)]

BACKUP slides

C_0, R_{10} at $\sqrt{s} = 7, 13 \text{ TeV}$, $Y \leq 4.8$, $\mu_F = r \sqrt{|\vec{k}_1||\vec{k}_2|}$



[F.G. C., D.Yu. Ivanov, B. Murdaca, A. Papa (2017)]

BACKUP slides

Looking for new observables

- BFKL feature: factorization between transverse and longitudinal (rapidities) degrees of freedom
 - Usual "growth with energy" signal mainly probes the longitudinal degrees of freedom
 - Mueller-Navelet correlation momenta mainly probe one of the transverse components, the azimuthal angles
- ! We would like to study observables for which the p_T (any p_T along the BFKL ladder) enters the game...
- ◊ ...to probe not only the general properties of the BFKL ladder, but also "to peek into the interior"...
 - ◊ ...by studying azimuthal decorrelations where the p_T of extra particles introduces a new dependence...

...multi-jet production!

BACKUP slides

Looking for new observables

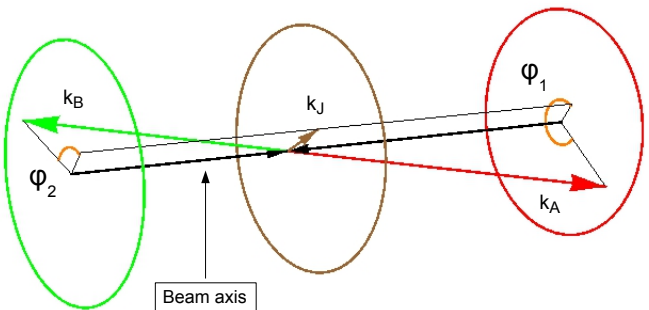
- BFKL feature: factorization between transverse and longitudinal (rapidities) degrees of freedom
 - Usual "growth with energy" signal mainly probes the longitudinal degrees of freedom
 - Mueller-Navelet correlation momenta mainly probe one of the transverse components, the azimuthal angles
- ! We would like to study observables for which the p_T (any p_T along the BFKL ladder) enters the game...
- ◊ ...to probe not only the general properties of the BFKL ladder, but also "to peek into the interior"...
 - ◊ ...by studying azimuthal decorrelations where the p_T of extra particles introduces a new dependence...

...multi-jet production!

[R. Maciula, A. Szczurek (2014, 2015)]
[I.K. Kutak, R. Maciula, M. Serino, A. Szczurek, A. van Hameren (2016)]

BACKUP slides

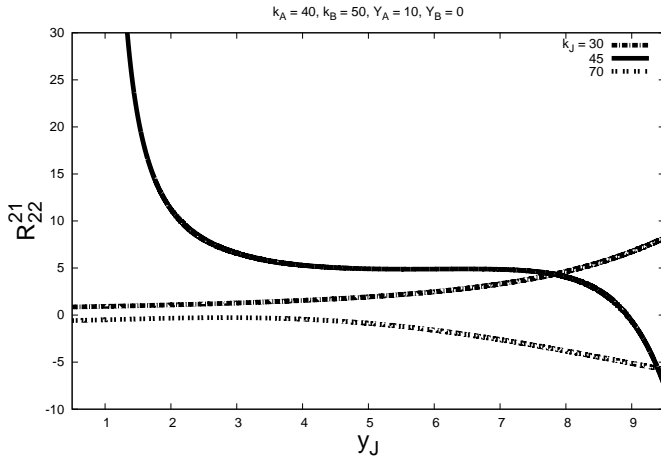
An event with three tagged jets



$$Y_B < y_J < Y_A$$

BACKUP slides

Partonic prediction of \mathcal{R}_{22}^{21} for $k_J = 30, 45, 70 \text{ GeV}$



[F. Caporale, G. Chachamis, B. Murdaca, A. Sabio Vera (2015)]

$Y_A - Y_B$ is fixed to 10; y_J varies between 0.5 and 9.5.

BACKUP slides

Next step: hadronic level predictions (3-jets)

- Introduce PDFs and running of the strong coupling:

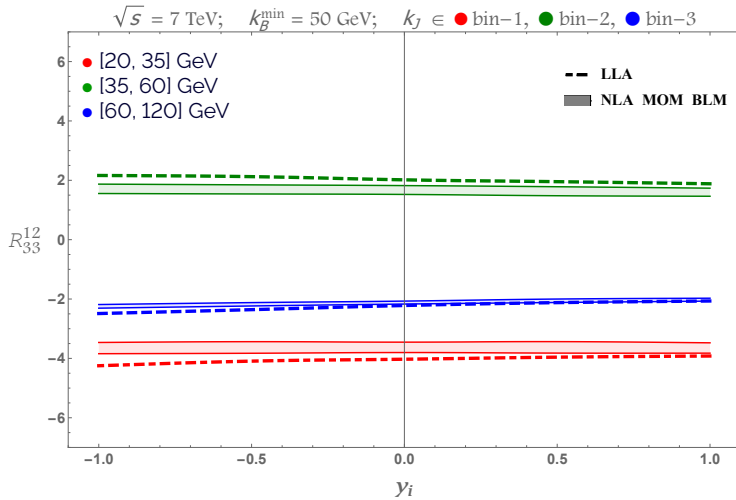
$$\frac{d\sigma^{\text{3-jet}}}{dk_A dY_A d\theta_A dk_B dY_B d\theta_B dk_J dy_J d\theta_J} = \frac{8\pi^3 C_F \bar{\alpha}_s(\mu_R)^3}{N_C^3} \frac{x_{J_A} x_{J_B}}{k_A k_B k_J} \int d^2 \vec{p}_A \int d^2 \vec{p}_B \delta^{(2)}(\vec{p}_A + \vec{k}_J - \vec{p}_B) \\ \times \left(\frac{N_C}{C_F} f_g(x_{J_A}, \mu_F) + \sum_{r=q,\bar{q}} f_r(x_{J_A}, \mu_F) \right) \\ \times \left(\frac{N_C}{C_F} f_g(x_{J_B}, \mu_F) + \sum_{s=q,\bar{q}} f_s(x_{J_B}, \mu_F) \right) \\ \times \varphi(\vec{k}_A, \vec{p}_A, Y_A - y_J) \varphi(\vec{p}_B, \vec{k}_B, y_J - Y_B)$$

- Match the LHC kinematical cuts (integrate $d\sigma^{\text{3-jet}}$ on k_T and rapidities):
 - ◊ 1. $k_A \geq 35 \text{ GeV}; k_B \geq 35 \text{ GeV}$; symmetric cuts
 - 2. $k_A \geq 35 \text{ GeV}; k_B \geq 50 \text{ GeV}$; asymmetric cuts
 - ◊ a) Y_A and Y_B integrated on windows
 - b) $Y_A - Y_B \equiv Y$ fixed
 - ◊ binning on y_J

BACKUP slides

a) $R_{33}^{12}(y_i)$ at 7 TeV

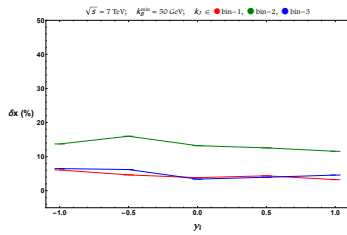
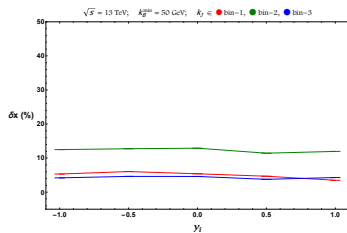
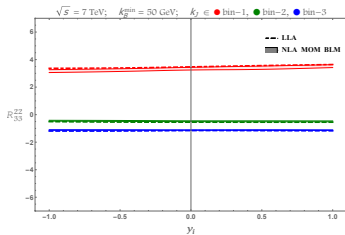
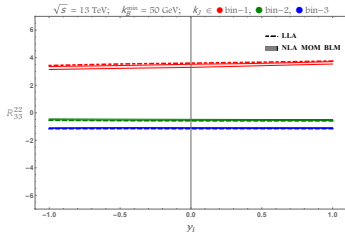
$k_A^{\min} = 35 \text{ GeV}$, $k_B^{\min} = 50 \text{ GeV}$, $k_A^{\max} = k_B^{\max} = 60 \text{ GeV}$ (asymmetric)



[I.F. Caporale, F.G. C., G. Chachamis, D. Gordo Gómez, A. Sabio Vera (2017)]

BACKUP slides

a) $R_{23}^{22}(y_i)$ at 13 and 7 TeV



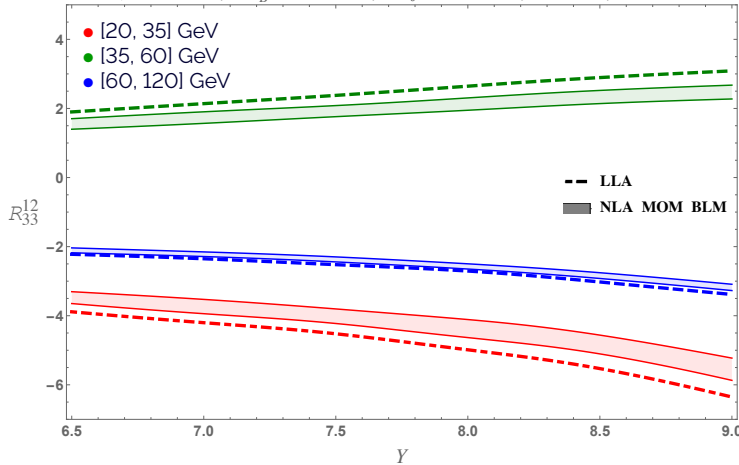
[F. Caporale, F.G. C., G. Chachamis, D. Gordo Gómez, A. Sabio Vera (2017)]

BACKUP slides

b) R_{33}^{12} vs Y at 7 TeV

$k_A^{\min} = 35 \text{ GeV}$, $k_B^{\min} = 50 \text{ GeV}$, $k_A^{\max} = k_B^{\max} = 60 \text{ GeV}$ (asymmetric)

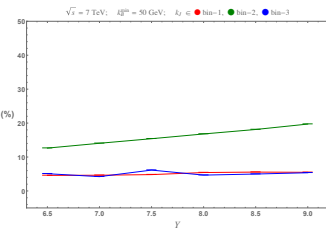
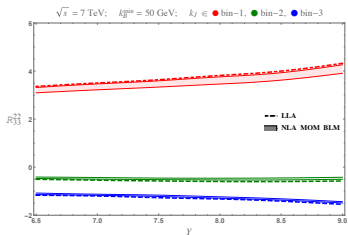
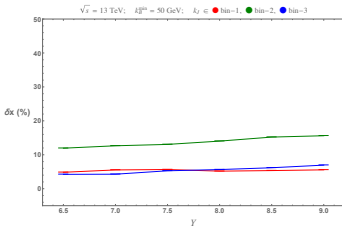
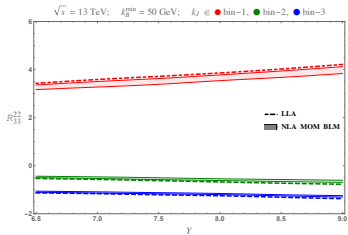
$\sqrt{s} = 7 \text{ TeV}$; $k_B^{\min} = 50 \text{ GeV}$; $k_J \in$ ● bin-1, ● bin-2, ● bin-3



[F. Caporale, F.G. C., G. Chachamis, D. Gordo Gómez, A. Sabio Vera (2017)]

BACKUP slides

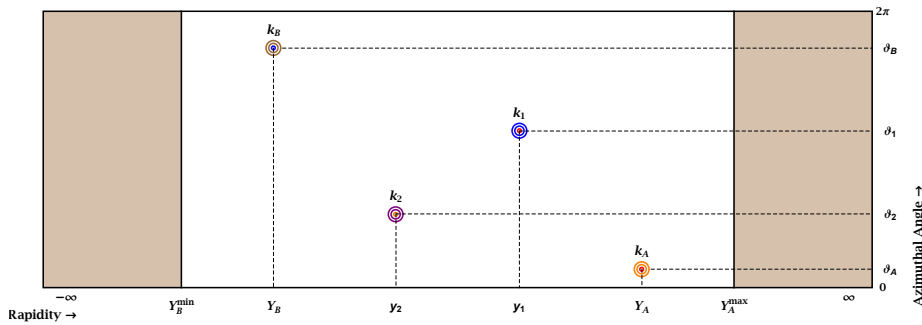
b) R_{23}^{22} vs γ at 13 and 7 TeV



[I.F.Caporale, F.G. C., G. Chachamis, D. Gordo Gómez, A. Sabio Vera (2017)]

BACKUP slides

A four-jet primitive lego-plot



$$Y_A^{\max} = -Y_B^{\min} = 4.7$$

BACKUP slides

Four-jets: generalized azimuthal coefficients - partonic level

$$\begin{aligned}\mathcal{C}_{MNL} &= \int_0^{2\pi} d\vartheta_A \int_0^{2\pi} d\vartheta_B \int_0^{2\pi} d\vartheta_1 \int_0^{2\pi} d\vartheta_2 \cos(M(\vartheta_A - \vartheta_1 - \pi)) \\ &\quad \cos(N(\vartheta_1 - \vartheta_2 - \pi)) \cos(L(\vartheta_2 - \vartheta_B - \pi)) \frac{d^6 \sigma^{4\text{-jet}}(\vec{k}_A, \vec{k}_B, Y_A - Y_B)}{dk_1 dy_1 d\vartheta_1 dk_2 d\vartheta_2 dy_2} \\ &= \frac{2\pi^2 \bar{\alpha}_s(\mu_R)^2}{k_1 k_2} (-1)^{M+N+L} (\tilde{\Omega}_{M,N,L} + \tilde{\Omega}_{M,N,-L} + \tilde{\Omega}_{M,-N,L} \\ &\quad + \tilde{\Omega}_{M,-N,-L} + \tilde{\Omega}_{-M,N,L} + \tilde{\Omega}_{-M,N,-L} + \tilde{\Omega}_{-M,-N,L} + \tilde{\Omega}_{-M,-N,-L})\end{aligned}$$

with

$$\begin{aligned}\tilde{\Omega}_{m,n,l} &= \int_0^{+\infty} dp_A p_A \int_0^{+\infty} dp_B p_B \int_0^{2\pi} d\Phi_A \int_0^{2\pi} d\Phi_B \\ &\quad \frac{e^{-im\Phi_A} e^{il\Phi_B} (p_A e^{i\Phi_A} + k_1)^n (p_B e^{-i\Phi_B} - k_2)^n}{\sqrt{(p_A^2 + k_1^2 + 2p_A k_1 \cos \Phi_A)^n} \sqrt{(p_B^2 + k_2^2 - 2p_B k_2 \cos \Phi_B)^n}} \\ &\quad \varphi_m(|\vec{k}_A|, |p_A|, Y_A - y_1) \varphi_l(|\vec{p}_B|, |\vec{k}_B|, y_2 - Y_B) \\ &\quad \varphi_n\left(\sqrt{p_A^2 + k_1^2 + 2p_A k_1 \cos \Phi_A}, \sqrt{p_B^2 + k_2^2 - 2p_B k_2 \cos \Phi_B}, y_1 - y_2\right)\end{aligned}$$

BACKUP slides

Four-jets: generalized azimuthal coefficients - partonic level

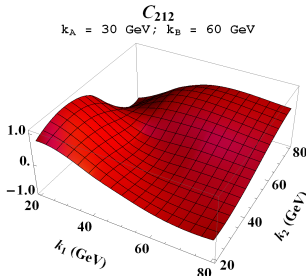
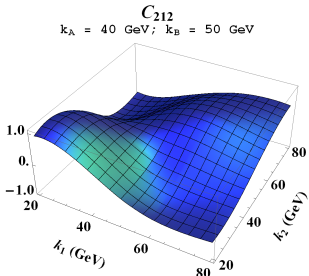
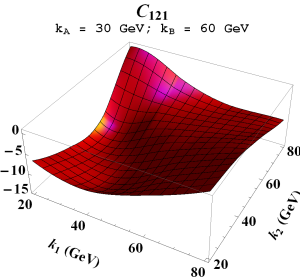
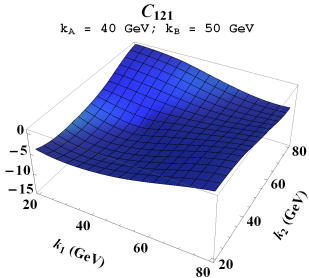
$$\mathcal{C}_{MNL} = \int_0^{2\pi} d\vartheta_A \int_0^{2\pi} d\vartheta_B \int_0^{2\pi} d\vartheta_1 \int_0^{2\pi} d\vartheta_2 \cos(M(\vartheta_A - \vartheta_1 - \pi)) \cos(N(\vartheta_1 - \vartheta_2 - \pi)) \cos(L(\vartheta_2 - \vartheta_B - \pi)) \frac{d^6 \sigma^{\text{4-jet}}(\vec{k}_A, \vec{k}_B, Y_A - Y_B)}{dk_1 dy_1 d\vartheta_1 dk_2 d\vartheta_2 dy_2}$$

Main observables: **generalized azimuthal correlation momenta**

$$\mathcal{R}_{PQR}^{MNL} = \frac{\mathcal{C}_{MNL}}{\mathcal{C}_{PRQ}} = \frac{\langle \cos(M(\vartheta_A - \vartheta_1 - \pi)) \cos(N(\vartheta_1 - \vartheta_2 - \pi)) \cos(L(\vartheta_2 - \vartheta_B - \pi)) \rangle}{\langle \cos(P(\vartheta_A - \vartheta_1 - \pi)) \cos(Q(\vartheta_1 - \vartheta_2 - \pi)) \cos(R(\vartheta_2 - \vartheta_B - \pi)) \rangle}$$

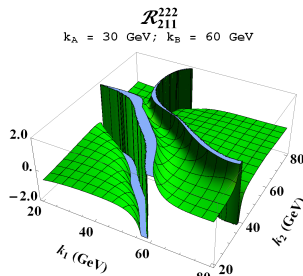
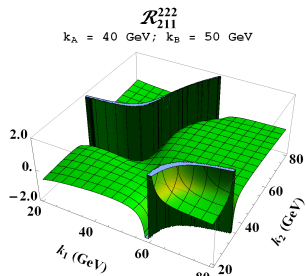
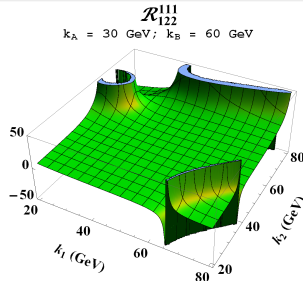
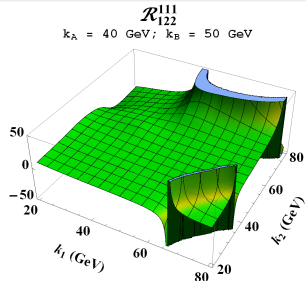
BACKUP slides

Partonic prediction of \mathcal{C}_{MNL} vs $k_{1,2}$ (4-jets)



BACKUP slides

Partonic prediction of \mathcal{R}_{PQR}^{MNL} vs $k_{1,2}$ (4-jets)



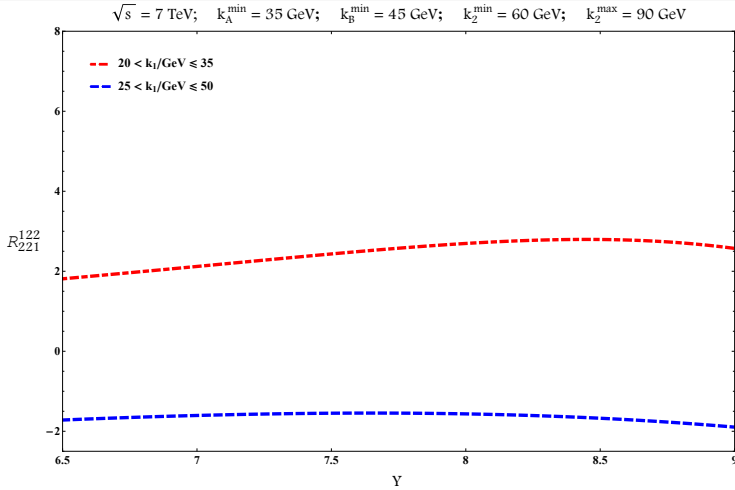
BACKUP slides

Next step: hadronic level predictions (4-jets)

- Introduce PDFs and running of the strong coupling
- Use realistic LHC kinematical cuts:
 - ◊ 1. $k_A^{\min} = 35 \text{ GeV}$, $k_A^{\max} = 60 \text{ GeV}$
 $k_B^{\min} = 45 \text{ GeV}$, $k_B^{\max} = 60 \text{ GeV}$
 $k_1^{\min} = 20 \text{ GeV}$, $k_1^{\max} = 35 \text{ GeV}$
 $k_2^{\min} = 60 \text{ GeV}$, $k_2^{\max} = 90 \text{ GeV}$
 - 2. $k_A^{\min} = 35 \text{ GeV}$, $k_A^{\max} = 60 \text{ GeV}$
 $k_B^{\min} = 45 \text{ GeV}$, $k_B^{\max} = 60 \text{ GeV}$
 $k_1^{\min} = 25 \text{ GeV}$, $k_1^{\max} = 50 \text{ GeV}$
 $k_2^{\min} = 60 \text{ GeV}$, $k_2^{\max} = 90 \text{ GeV}$
- ◊ $Y = Y_A - Y_B$ fixed;
 $Y_A - y_1 = y_1 - y_2 = y_2 - Y_B = Y/3$
- ◊ $\sqrt{s} = 7, 13 \text{ TeV}$

BACKUP slides

R_{221}^{122} at $\sqrt{s} = 7$ TeV vs $Y = Y_A - Y_B$ for two k_1 bins



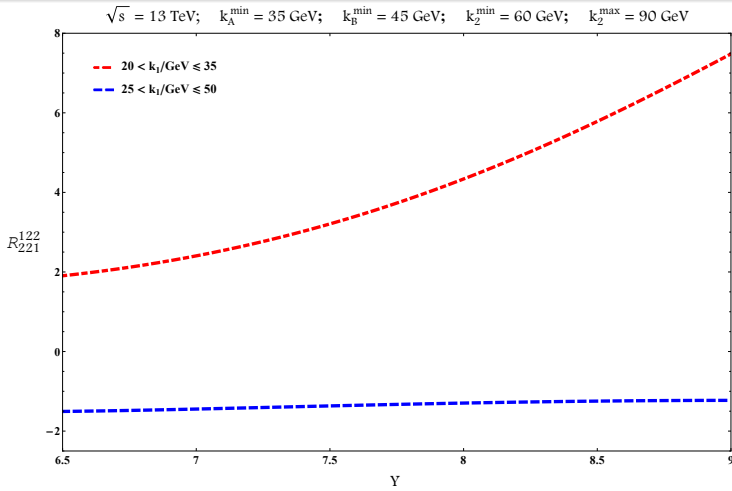
[I.F. Caporale, F.G. C., G. Chachamis, D. Gordo Gómez, A. Sabio Vera (2016)]

Y is the rapidity difference between the most forward/backward jet;

$$Y_A - y_1 = y_1 - y_2 = y_2 - Y_B = Y/3.$$

BACKUP slides

R_{221}^{122} at $\sqrt{s} = 13$ TeV vs $\Upsilon = \Upsilon_A - \Upsilon_B$ for two k_1 bins



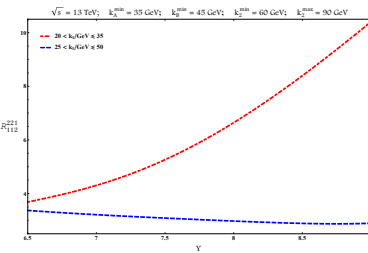
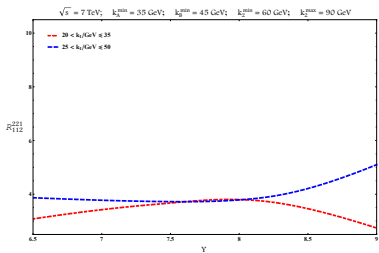
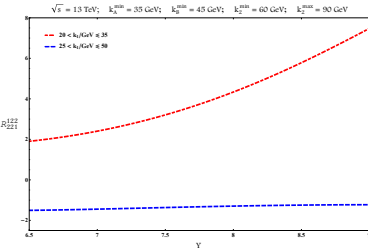
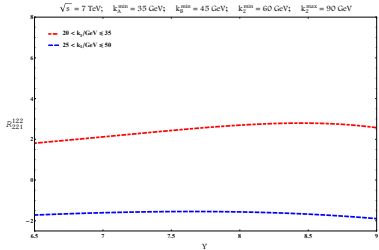
[F. Caporale, F.G. C., G. Chachamis, D. Gordo Gómez, A. Sabio Vera (2017)]

Υ is the rapidity difference between the most forward/backward jet;

$$\Upsilon_A - y_1 = y_1 - y_2 = y_2 - \Upsilon_B = \Upsilon/3.$$

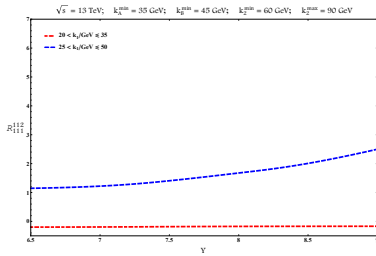
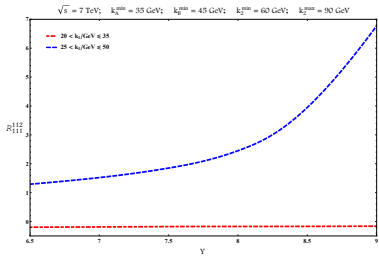
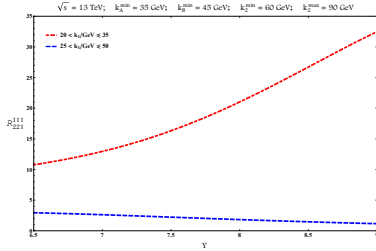
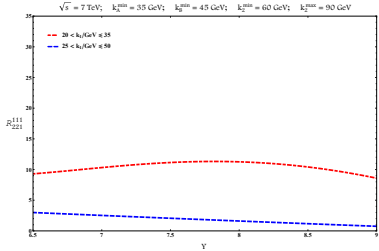
BACKUP slides

R_{221}^{122} and R_{112}^{221} vs $Y = Y_A - Y_B$ and \sqrt{s} for two k_1 bins



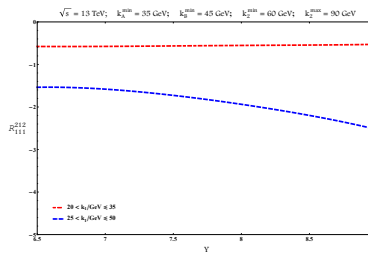
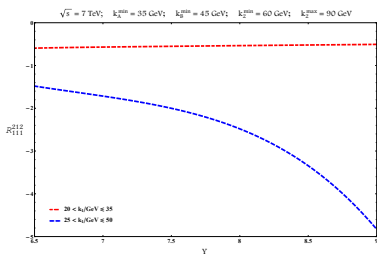
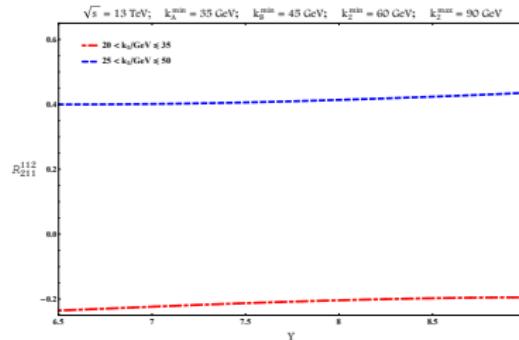
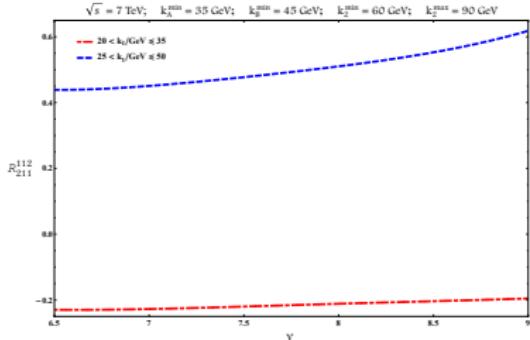
BACKUP slides

R_{221}^{111} and R_{111}^{112} vs $Y = Y_A - Y_B$ and \sqrt{s} for two k_1 bins



BACKUP slides

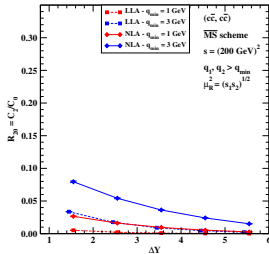
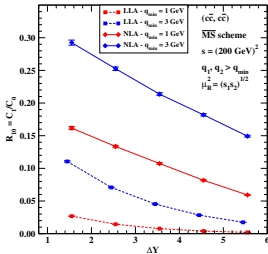
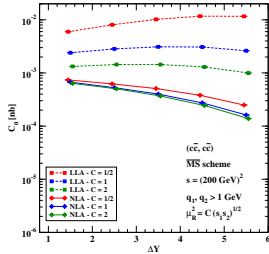
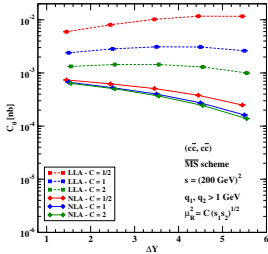
R_{211}^{112} and R_{111}^{212} vs $\Upsilon = \Upsilon_A - \Upsilon_B$ and \sqrt{s} for two k_1 bins



[F. Caporale, F.G. C., G. Chachamis, D. Gordo Gómez, A. Sabio Vera (2017)]

BACKUP slides

C_0 and R_{n0} vs γ at LEP2 (heavy-quarks)

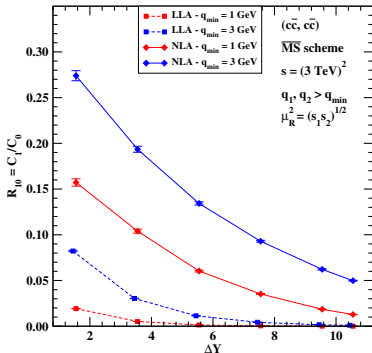
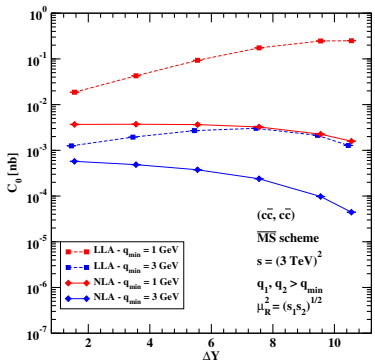


$$s_{1,2} = m_{1,2}^2 + q_{1,2}^2$$

I.F.G. C., D.Yu. Ivanov, B. Murdaca, A. Papa (2017) arXiv:1709.10032 [hep-ph]

BACKUP slides

C_0 and R_{10} vs γ at e^+e^- future colliders (heavy-quarks)

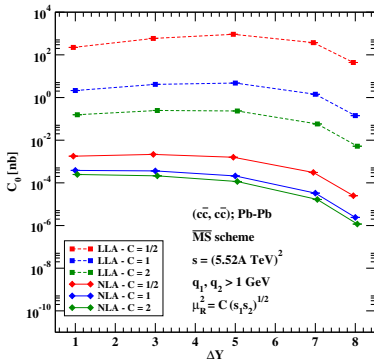
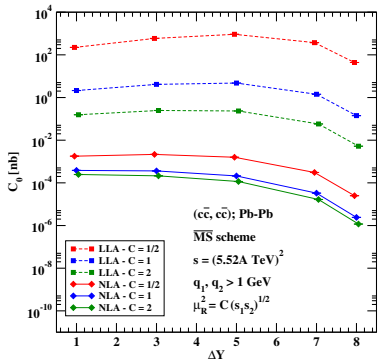


$$s_{1,2} = m_{1,2}^2 + q_{1,2}^2$$

I.F.G. C., D.Yu. Ivanov, B. Murdaca, A. Papa (2017) arXiv:1709.10032 [hep-ph]

BACKUP slides

C_0 vs Υ in Pb-Pb UPC collisions at LHC (heavy-quarks)



$$s_{1,2} = m_{1,2}^2 + q_{1,2}^2$$

I.F.G. C., D.Yu. Ivanov, B. Murdaca, A. Papa (2017) arXiv:1709.10032 [hep-ph]